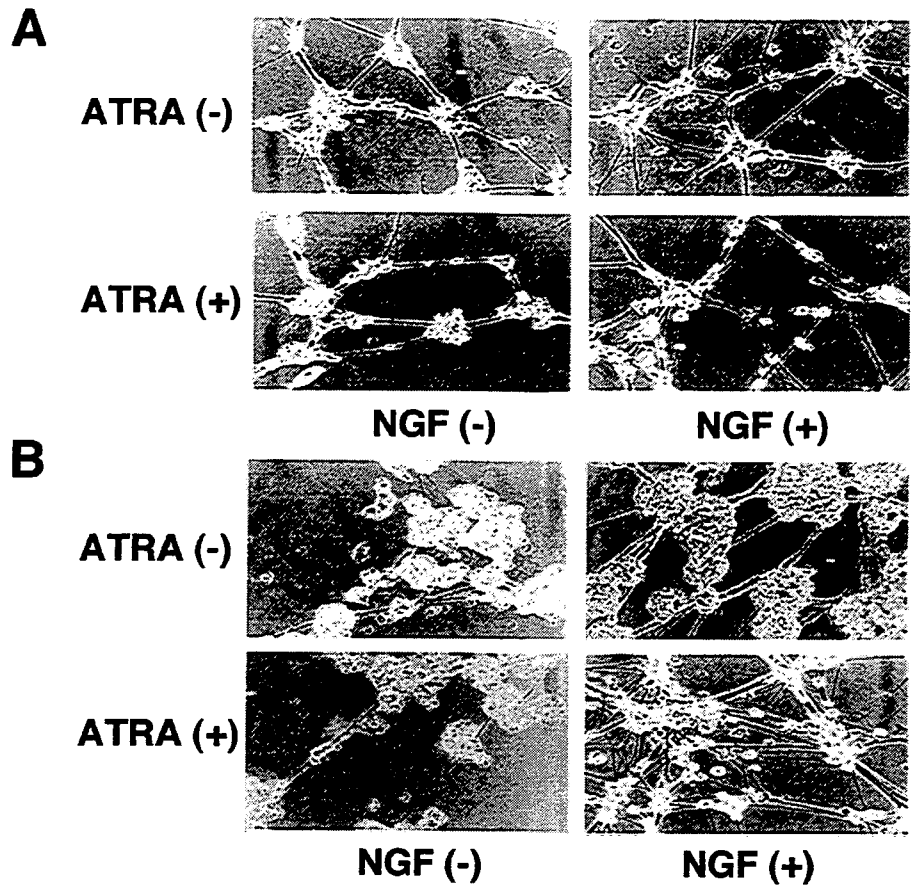

Figure 3. Neurite extension of primary neuroblastomas in response to NGF and/or ATRA. Total cell suspensions (A) and CD3- and CD19-negative non-adherent cells (B) prepared from case 625 were treated with or without the indicated combinations of NGF (100 ng/ml) and ATRA (5 μM) for seven days, and their neurite outgrowth was examined.

to immunohistochemical staining with anti-NB84 antibody. As shown in Fig. 2C, NB84-positive neuroblastoma cells were efficiently enriched by our present procedure.

Neurite extension in response to ATRA and/or NGF. To address whether magnetic bead-mediated enrichment of neuroblastoma cells could affect their biological behavior, we compared the degree of neurite outgrowth between cells before and after the selection. To this end, total cell suspensions and CD3- and CD19-negative non-adherent cells prepared from case 625 were cultured in the presence or absence of ATRA and/or NGF. Seven days after treatment, cells were observed with a phase-contrast microscope. Representative data are shown in Fig. 3A and B. ATRA alone had undetectable effects on both cells, whereas NGF treatment led to a formation of neurites in both cells. To note, treatment of CD3- and CD19-negative non-adherent cells with the combination of ATRA and NGF significantly enhanced neurite outgrowth as compared with total cell suspensions, suggesting that NB84-positive neuroblastoma cells purified by magnetic bead-mediated separation retain the biological properties of primary neuroblastomas.

Discussion

To understand the biological properties of neuroblastomas *in vivo*, it is necessary to isolate neuroblastoma cells from fresh neuroblastoma tissues in culture. As described previously (18), growth factors have an ability to promote proliferation or differentiation of neuroblastoma cells through interactions with their specific receptors. Among them, NGF, which induces normal adrenal cells to differentiate into cells identical to sympathetic neurons, plays a key role in the development of neuroblastomas (19). It has been well established that the high-affinity NGF receptor *TrkA* gene is highly expressed in low-stage neuroblastomas but not in advanced neuroblastomas (4). Several lines of evidence suggest that NGF responsiveness of neuroblastoma-derived cell lines is closely associated with the expression levels of *TrkA* and the low-affinity NGF receptor gene $p75^{NTR}$ (20,21). Since $p75^{NTR}$ alone had undetectable effects on NGF responsiveness of neuroblastoma cell lines (22), we sought to isolate neuroblastoma cells from primary neuroblastoma tissues by using magnetic beads coated with anti-$p75^{NTR}$ antibody. Under our experimental conditions, we failed to enrich neuroblastoma cells due to diverse expression levels of $p75^{NTR}$ in primary neuroblastoma samples (data not shown).

During the preparation of primary neuroblastoma samples, we noticed that primary neuroblastoma tissues contain substantial amounts of lymphocytes. We then employed magnetic beads coated with anti-CD3 or anti-CD19 antibody to remove lymphocytes from primary neuroblastoma samples. After magnetic separation, the unbound materials were cultured overnight and the non-adherent cells were collected.

Table I. FACS analysis of advanced neuroblastomas.

			Total cell suspension				Cells after treatment with beads		
			Lymphocytes			NB cells	Lymphocytes		NB cells
Case	Age	Stage	Total (%)	CD3 (%)	CD19 (%)	NB84 (%)	CD3 (%)	CD19 (%)	NB84 (%)
548	2 years	4	4	4	0	ND	ND	ND	ND
559	1 year	3	20	20	0	ND	0	0	ND
564	2 years	4	20	7	13	ND	0	0	ND
580	9 months	3	21	9	12	ND	ND	ND	ND
581	1 year	4	31	31	0	ND	ND	ND	ND
602	1 year	4	13	13	0	17	0	0	50
603	2 years	4	15	4	11	ND	ND	ND	ND
613	4 years	4	56	28	28	16	0	0	51
615	7 months	3	15	11	4	ND	0	0	ND
649	6 years	4	0	0	0	22	0	0	56

ND, not determined.

Table II. FACS analysis of neuroblastomas in stages 1, 2 and 4s.

			Total cell suspension				Cells after treatment with beads		
			Lymphocytes			NB cells	Lymphocytes		NB cells
Case	Age	Stage	Total (%)	CD3 (%)	CD19 (%)	NB84 (%)	CD3 (%)	CD19 (%)	NB84 (%)
601	9 months	2	28	20	8	ND	ND	ND	ND
609	7 months	1	58	44	14	ND	0	0	ND
611	7 months	4s	57	57	0	ND	0	0	ND
619	9 months	2	83	72	11	50	0	0	ND
624	8 months	1	96	48	48	ND	40	34	ND
625	7 months	1	41	41	0	66	0	0	72
627	7 months	1	15	15	0	0	0	0	ND
641	7 months	1	0	0	0	64	0	0	65
643	1 year	1	0	0	0	78	0	0	86
678	7 months	1	15	14	1	86	2	0	95
684	8 months	1	4	4	0	95	0	0	97
687	8 months	1	11	10	1	86	2	1	75
711	7 months	1	20	19	1	79	0	0	95
716	8 months	1	20	18	2	22	2	1	60

ND, not determined.

FACS analysis revealed that our procedure successfully enriches NB84-positive viable neuroblastoma cells (Tables I and II), indicating that NB84-positive neuroblastoma cells can be separated from Schwann cells as well as from fibroblasts by taking advantage of their differential adhesion. Moreover, NB84-positive neuroblastoma cells responded to ATRA and NGF, suggesting that our enriched materials retained the biological properties of primary neuroblastomas. Collectively, our magnetic bead-mediated isolation system provides fresh and enriched neuroblastoma cells in culture.

Acknowledgements

This study was supported in part by a Grant-in-Aid from the Ministry of Health, Labour and Welfare for Third Term Comprehensive Control Research for Cancer, a Grant-in-Aid for Scientific Research on Priority Areas from the Ministry of Education, Culture, Sports, Science and Technology, Japan, a Grant-in-Aid for Scientific Research from Japan Society for the Promotion of Science and Uehara Memorial Foundation.

References

1. Brodeur GM: Neuroblastoma: biological insights into a clinical enigma. Nat Rev Cancer 3: 203s216, 2003.
2. Schor NF: Neuroblastoma as a neurobiological disease. J Neurooncol 41: 159-166, 1999.
3. Brodeur GM and Nakagawara A: Molecular basis of clinical heterogeneity in neuroblastoma. Am J Pediatr Hematol Oncol 14: 111-116, 1992.
4. Nakagawara A, Arima-Nakagawara M, Scavarda NJ, Azar CG, Cantor AB and Brodeur GM: Association between high levels of expression of the TRK gene and favorable outcome in human neuroblastoma. N Engl J Med 328: 847-854, 1993.
5. Nakagawara A, Azar CG, Scavarda NJ and Brodeur GM: Expression and function of TRK-B and BDNF in human neuroblastomas. Mol Cell Biol 14: 759-767, 1994.
6. Brodeur GM, Nakagawara A, Yamashiro DJ, Ikegaki N, Liu XG, Azar CG, Lee CP and Evans AE: Expression of TrkA, TrkB and TrkC in human neuroblastomas. J Neurooncol 31: 49-55, 1997.
7. Chen S, Caragine T, Cheung NK and Tomlinson S: Surface antigen expression and complement susceptibility of differentiated neuroblastoma clones. Am J Pathol 156: 1085-1091, 2000.
8. Seeger RC, Rayner SA, Banerjee A, Chung H, Laug WE, Neustein HB and Benedict WF: Morphology, growth, chromosomal pattern and fibrinolytic activity of two new human neuroblastoma cell lines. Cancer Res 37: 1364-1371, 1977.
9. Ross RA, Spengler BA and Chang TD: Transdifferentiation of neuroblastoma cells. J Natl Cancer Inst 71: 741-747, 1983.
10. Spengler BA, Lazarova DL, Ross BA and Biedler JL: Cell lineage and differentiation state are primary determinants of MYCN gene expression and malignant potential in human neuroblastoma cells. Oncol Res 9: 467-476, 1997.
11. Ciccarone V, Spengler BA, Meyers MB, Biedler JL and Ross RA: Phenotypic diversification in human neuroblastoma cells: expression of distinct neural crest lineages. Cancer Res 49: 219-225, 1989.
12. Biedler JL, Spengler BA and Ross RA: Transdifferentiation of human neuroblastoma cells results in coordinate loss of neuronal and malignant properties. Prog Clin Biol Res 271: 265-276, 1988.
13. Brodeau GM, Pritchard J, Berthold F, Carlsen NL, Castel V, Castelberry RP, De Bernardi B, Evans AE, Favrot M, Hedborg F, Kaneko M, Kemshead J, Lampert F, Lee RE, Look AT, Pearson AD, Philip T, Roald B, Sawada T, Seegel RC, Tsuchida Y and Voute PA: Revisions of the international criteria for neuroblastoma diagnosis, staging, and response to treatment. J Clin Oncol 11: 1466-1477, 1993.
14. Matsumura T, Iehara T, Sawada T and Tsuchida Y: Prospective study for establishing the optimal therapy of infantile neuroblastoma in Japan. Med Pediatr Oncol 31: 210, 1998.
15. Kaneko M, Nishihara H, Mugishima H, Ohnuma N, Nakada K, Kawa K, Fukuzawa M, Suita S, Sera Y and Tsuchida Y: Stratification of treatment of stage 4 neuroblastoma patients based on N-myc amplification status: study group of Japan for treatment of advanced neuroblastoma. Med Pediatr Oncol 31: 1-7, 1998.
16. Bomken SN, Redfern K, Wood KM, Reid MM and Tweddle DA: Limitations in the ability of NB84 to detect metastatic neuroblastoma cells in bone marrow. J Clin Pathol 59: 927-929, 2006.
17. Thomas JO, Nijjar J, Turley H, Micklem K and Gatter KC: NB84: a new monoclonal antibody for the recognition of neuroblastoma in routinely processed material. J Pathol 163: 69-75, 1991.
18. Janet T, Ludecke G, Otten U and Unsicker K: Heterogeneity of human neuroblastoma cell lines in their proliferative responses to basic FGF, NGF, and EGF: correlation with expression of growth factors and growth factor receptors. J Neurosci Res 40: 707-715, 1995.
19. Nakagawara A: The NGF story and neuroblastoma. Med Pediatr Oncol 31: 113-115, 1998.
20. Sonnenfeld KH and Ishii DH: Nerve growth factor effects and receptors in cultured human neuroblastoma cell lines. J Neurosci Res 8: 375-391, 1982.
21. Chen J, Chattopadhyay B, Venkatakrishnan G and Ross AH: Nerve growth factor-induced differentiation of human neuroblastoma and neuroepithelioma cell lines. Cell Growth Differ 1: 79-85 1990.
22. Chen J, Liu TH and Ross AH: Expression of recombinant NGF receptor in human neuroblastoma cell line without NGF receptor. Basic Med Sci Clin 11: 26-31, 1991.

Silencing Ku80 using small interfering RNA enhanced radiation sensitivity *in vitro* and *in vivo*

YOSHINORI NIMURA[1,6], TETSUYA KAWATA[2], KATSUHIRO UZAWA[3], JUNKO OKAMURA[2], CUIHUA LIU[2], MASAYOSHI SAITO[2], HIDEAKI SHIMADA[1,4], NAOHIKO SEKI[1,5], AKIRA NAKAGAWARA[6], HISAO ITO[2], TAKENORI OCHIAI[1,4] and HIDEKI TANZAWA[1,3]

[1]21st Century Center of Excellence Program, [2]Department of Radiology, [3]Clinical Molecular Biology, [4]Academic Surgery, and [5]Functional Genomics, Chiba University Graduate School of Medicine; [6]Division of Biochemistry, Chiba Cancer Center Research Institute, Chiba, Japan

Received February 5, 2007; Accepted March 21, 2007

Abstract. Ku80 is an important component of DNA double-strand break repair, and Ku80 deficiency leads to extreme sensitivity to ionizing radiation. We studied whether radiation therapy combined with Ku80 silencing by small interfering RNA enhances radiation sensitivity *in vitro* and *in vivo*. Seven human cancer cell lines were transfected with Ku80 siRNA included in hemagglutinating virus of Japan envelope vector. H1299 cells were implanted into male BALB/C nu/nu nude mice treated with Ku80 siRNA and irradiation. The survival rate of cell lines transfected with Ku80 siRNA decreased by 10% to 26% with 2-Gy irradiation compared with untransfected cell lines. The gamma-H2AX phosphorylation-positive rates of Ku80 siRNA combined treatment 0.5 h after irradiation in A549 cells and 6 h in H1299 cells were significantly higher (77.6%, p=0.033 and 76.7%, p=0.026, respectively), compared with the groups not treated with siRNA. H1299 xenograft tumors treated with combined therapy decreased in volume and re-grew slowly compared with radiation alone. Our results indicate that combined therapy consisting of Ku80 siRNA and irradiation contributes to inhibition of tumor growth and may be a novel strategy for cancer treatment.

Correspondence to: Professor Hideki Tanzawa, 21st Century Center of Excellence Program, Chiba University Graduate School of Medicine, 1-8-1 Inohana, Chuo-ku, Chiba 260-8677, Japan
E-mail: tanzawap@faculty.chiba-u.jp

Abbreviations: DSBs, double-strand breaks; NHEJ, non-homologous end-joining; DNA-PKcs, DNA-dependent protease kinase catalytic subunits; siRNA, small interfering RNA; HVJ, hemagglutinating virus of Japan; HVJ-E, HVJ envelope; PBS, phosphate-buffered saline; xrs-5, X-ray-sensitive mutant 5; CHO K1, Chinese hamster ovary

Key words: Ku80, small interfering RNA, HVJ envelope, radiation sensitivity

Introduction

Radiation therapy is a standard treatment for patients with many kinds of cancers. Therapeutic strategies and protocols have been developed and the effectiveness of radiation therapy has greatly improved. However, it is difficult to predict the efficacy and side effects before therapy. Even in patients with the same stage of carcinoma, different responses and resistance to radiation therapy frequently affect the therapy. Radiation therapy with enhanced efficacy using a molecular technique is not yet established. A novel strategy based on a biologic mechanism should optimize the treatment of patients with carcinoma.

DNA double-strand breaks (DSBs) are potentially lethal DNA lesions induced by ionizing radiation (1,2). DSBs can be repaired by homologous recombination or non-homologous end-joining (NHEJ) (1,2). In mammals, NHEJ is especially important for repairing radiation-induced DSBs. Several factors, including Ku70, Ku80, DNA-dependent protease kinase catalytic subunits (DNA-PKcs), artemis, X-ray-complementation group 4, and DNA ligase IV, participate in this pathway (3-5). Ku works in a comparatively early stage. The Ku70/80 complex binds to the DSB ends, recruits DNA-PKcs, and initiates repair (3,6). Ku deficiency leads to extreme sensitivity to radiation (7,8).

Small interfering RNA (siRNA), has been used widely to silence gene expression, and has been evaluated as an attractive tool for use in therapeutics of many cancers (9-14). Some studies have reported that silencing the various repair genes, *ATM*, *ATR*, and *DNA-PKcs* (15,16), *Rad51* (17), *NBS1* (18,19), and *Mre11* (20), increased radiation sensitivity. However, the efficacy of Ku80 silencing for radiation sensitivity has not yet been evaluated.

siRNA technology is a powerful method of gene down-regulation; however, *in vivo*, it has been difficult to achieve high efficacy using the siRNA delivery system. The hemagglutinating virus of Japan (HVJ; Sendai virus) envelope vector is a new reagent for the transfection of DNA, protein, and oligonucleotides (21-26). The HVJ envelope (HVJ-E) vector was constructed with inactivated particles and therefore has no viral activity. Using the HVJ-E system, the efficiency of

gene transfer into various cell lines is greatly enhanced, even when injected into organs directly in *in vivo* experiments (21-23).

We hypothesized that radiation therapy combined with Ku80 silencing might enhance radiation sensitivity, because of the reduced reparative ability of DSBs. In the current study, the expression of Ku80 was alternately inhibited using siRNA included in HVJ-E, and we studied *in vitro* and *in vivo* whether radiation sensitivity could be enhanced regardless of the type and radiation survival rate of the cancer cell lines.

Materials and methods

Cell lines and treatment. A549 and H1299 cells, which are lung carcinomas, were obtained from the American Type Culture Collection (Rockville, MD). A549 cells express normal p53, and H1299 cells are null for the *p53* gene. TE13 (esophageal carcinoma), PANC-1 (pancreas carcinoma), MIAPaCa-2 (pancreas carcinoma), DU-145 (prostate carcinoma), and ME-180 (cervical carcinoma) cells were obtained from the Cell Resource Center for Biomedical Research Institute of Development, Aging and Cancer Tohoku University (Miyagi, Japan). All cells were maintained as a monolayer in Dulbecco's modified Eagle's medium (Sigma, St. Louis, MO), supplemented with 10% fetal bovine serum, and grown at 37°C in a humidified atmosphere of 5% carbon dioxide. Exponentially grown cells were used for all experiments.

Clonogenic assay. To evaluate radiation sensitivity, surviving fractions were measured using a standard colony-formation assay (27). Briefly, the cells were counted and the appropriate number seeded into 60-mm dishes in triplicate for each dose. Six hours later, when all cells had attached but not yet divided, the cells were irradiated with doses ranging from 0 to 6-Gy using an MBR-1520R-3 (Hitachi, Tokyo, Japan) generator operated under 150 kVp and 20 mA with a 1-mm aluminum filter. The dose rate was about 2-Gy/minute. Colonies obtained after 10 to 14 days were stained with crystal violet and contained >50 cells.

siRNA transfection. The siRNA used for Ku80 gene silencing was designed by Qiagen (Valencia, CA). The target sequence was AAG CGA GTA ACC AGC TCA TAA, and the siRNA sense sequence was r(GCG AGU AAC CAG CUC AUA A)dTdT.

Transfection of Ku80 siRNA was conducted with HVJ-E according to the manufacturer's recommendations (Ishihara Sangyo Kaisha, Ltd., Osaka, Japan). Briefly, cells were seeded into 6-well plates for 24 h before siRNA transfection. One microgram of siRNA was prepared to make complexes with HVJ-E according to the manufacturer's instructions (Ishihara Sangyo Kaisha, Ltd.). Several cell lines were transfected with Ku80 siRNA included in HVJ-E in medium supplemented with 10% fetal bovine serum. Forty hours after transfection, the cells were trypsinized and some were irradiated for clonogenic assay. The rest of the cells were lysed to extract protein for Western blotting.

Western blot analysis. Cells were lysed in lysis buffer [50 mM Tris-HCl (pH 8.0), 450 mM NaCl, 1% Triton X-100, 1 mM EDTA (pH 8.0), and 0.6 mM PMSF] containing a protein inhibitor cocktail (4-benzenesulfonyl, fluoride, pepstatin A, E-64, bestatin, leupeptin, and aprotinin) (Sigma). Protein concentrations of lysates were determined using a protein assay kit (Bio-Rad, Hercules, CA). Forty micrograms of protein was loaded and electrophoresed on 10% sodium dodecyl sulfate polyacrylamide gels. After blotting the nitrocellulose membranes, the protein was probed with primary mouse monoclonal Ku70, Ku80 (Santa Cruz Biotechnology, Inc., Santa Cruz, CA), and ß-actin (Sigma) antibodies then with secondary horseradish peroxidase-conjugated goat anti-mouse IgG antibody (Santa Cruz Biotechnology, Inc.). The immunoreactive bands were visualized using enhanced chemiluminescence on X-ray film (ECL Western Blotting Detection Reagent, GE Healthcare Bio-Sciences Corp., Piscataway, NJ).

Immunofluorescent staining for gamma-H2AX. Cells were seeded onto chamber slides (Nalge Nunc International, Naperville, IL) and transfected with the HVJ-E vector containing Ku80 siRNA for 40 h according to the manufacturer's instructions (Ishihara Sangyo Kaisha, Ltd.). After transfection, the cells were irradiated with 2-Gy or treated immediately without irradiation. Irradiated cells were treated using the following procedure after 30 min or 6 h. The cells were fixed with 1% paraformaldehyde solution in phosphate-buffered saline (PBS) for 30 min at room temperature, soaked in -20°C 99% methanol for 5 min, and incubated in 3% bovine serum albumin with 0.2% Tween-20 in PBS for 1 h at 37°C. The cells were probed in primary mouse monoclonal anti-phospho-H2A.X (ser139) antibody (Upstate Biotechnology, Lake Placid, NY) at a dilution of 1:300 for 1.5 h at 37°C and then in secondary Cy2-goat anti-rabbit IgG antibody at a dilution of 1:400 for 1 h at room temperature.

Fluorescence images were captured by Axioskop2 plus confocal microscopy equipped with a CCD camera and quantitated using AxioVisio Release 4.3 software (Carl Zeiss, Oberkochen, Germany). Significant colocalization of nuclear foci was determined by visualization of green spots on a DAPI background.

Gamma-H2AX foci were determined in five fields and at least 50 cells of each experiment. The cells were classified as positive when more than 10 foci were counted in the nucleus.

In vivo xenograft model. In vivo studies were carried out in accordance with the Guidelines for Animal Experimentation of Chiba University. Four-week-old male BALB/C nu/nu nude mice were obtained from Charles River Japan Inc. (Yokohama, Japan). To generate tumor xenografts, 5.0×10^6 viable H1299 cells were subcutaneously injected into the right hind legs. Tumors were measured in two dimensions with calipers and the volume was estimated using the following calculation: (major axis) x (minor axis) x (minor axis) x 1/2.

We generated two protocols, one for one fraction and the other for five fractions. For one fraction, when the tumors reached 150-200 mm^3 (day 0), the mice were randomly divided into three groups: control (no radiation; n=11), radiation alone (4-Gy in one fraction on day 1; n=6), and Ku80 siRNA treatment with radiation (siRNA injection on day 0 and 4-Gy in one fraction on day 1; n=6). For five

fractions, when the tumors reached 750-1000 mm^3 (day 0), the mice were randomly divided into three groups: control (no radiation; n=10), radiation alone (4-Gy in one fraction on days 1, 2, 3, 4, and 5; n=7), and Ku80 siRNA treatment with radiation (siRNA injection on days 2 and 4, and 4-Gy in one fraction on days 1, 2, 3, 4, and 5; n=8).

Gene delivery. H1299 xenograft tumors in the hind legs of nude mice were treated with Ku80 siRNA included in HVJ-E. The HVJ-E complex included Ku80 siRNA prepared as previously described. Ku80 siRNA was injected directly into the tumors. Each injection was diluted in a total volume of 50 μl of 0.9% sodium chloride solution and administered in one pass using a 27-gauge needle.

Statistical analysis. Statistical analysis was performed using SigmaStat 3.1 (Point Richmond, CA). For a single comparison, the level of statistical significance was confirmed using Student's t test. $p<0.05$ were considered statistically significant.

Results

Down-regulation of Ku80 protein expression by siRNA in A549 and H1299 cells. To determine whether Ku80 silencing contributes to radiation sensitivity, two siRNAs were designed and screened for the ability to down-regulate target protein expression. To determine the best protocol for silencing Ku80 protein expression, the cells were transfected with siRNA/HVJ-E complexes at various times, and protein extracts were obtained from 6 to 96 h after transfection. Western blot analyses showed that siRNA/HVJ-E complexes minimized Ku80 expression 40 h after transfection compared with untransfected cells (data not shown). We used 40 h of treatment with siRNA for the experiments.

Western blot analysis of Ku80 protein expression in A549 and H1299 cells was performed 40 h after transfection with Ku80 siRNA (Fig. 1A). Ku80 protein expression was suppressed, indicating successful gene silencing by siRNA. In cells transfected with Ku80 siRNA, Ku80 protein decreased compared with the transfected HVJ-E or the untransfected cells. Interestingly, although the cells were transfected with Ku80 siRNA, Ku70 protein expression also was suppressed and correlated with Ku80 expression level in both cell lines. The A549 cells are wild-type cells of the *p53* gene and the H1299 cells are the null type. The efficiency of the suppression did not depend on the *p53* gene status.

Cellular sensitivity after treatment with Ku80 siRNA. The A549 and H1299 cells exhibited a typical clonogenic survival curve with a shoulder signifying cellular repair capacity. Doses of 2, 4, and 6-Gy of irradiation alone killed about 31, 60, and 84% of the A549 cells, and 21, 53, and 76% of the H1299 cells, respectively (Fig. 1B). Furthermore, the survival rates of cells transfected with HVJ-E alone were close to the rate for the original cells. However, Ku80 siRNA enhanced cell killing in 57, 86, and 96% of the A549 cells and 35, 71, and 90% of the H1299 cells, respectively. siRNA inhibition of Ku80 protein confirmed enhanced radiation sensitivity in siRNA-transfected cells compared with the transfected

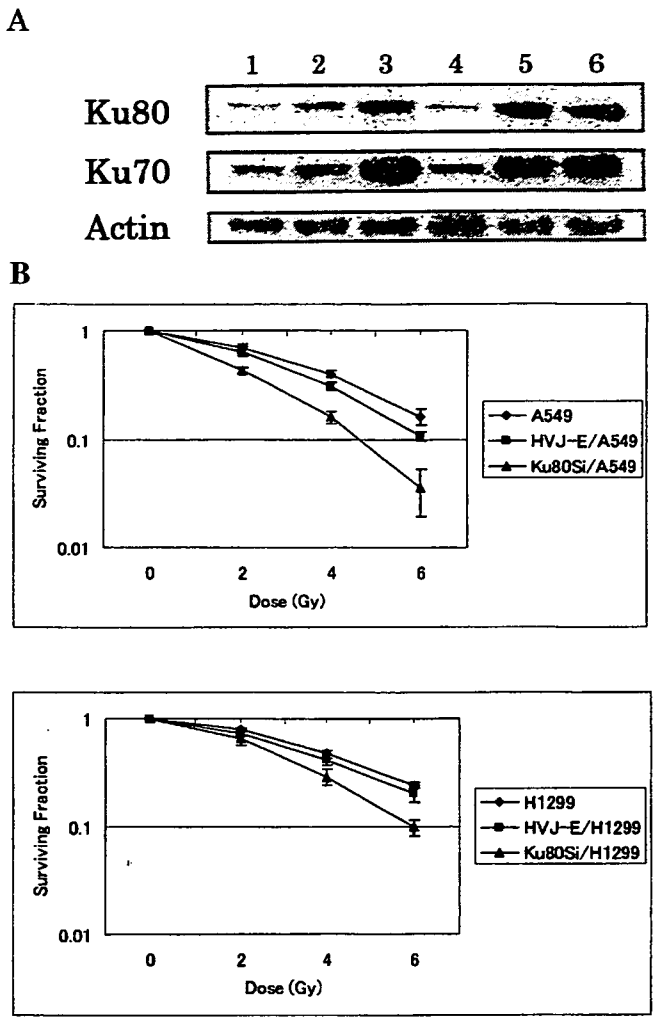

Figure 1. Down-regulation of Ku80 protein and radiation sensitivity in A549 and H1299 cells. Western blotting: after treatment with HVJ-E including Ku80 siRNA for 40 h, the protein expression of Ku80 is suppressed compared with the cell lines without siRNA or those treated with only HVJ-E. Actin serves as a loading control. Lane 1, Ku80si/A549; lane 2, HVJ-E/A549; lane 3, A549; lane 4, Ku80si/H1299; lane 5, HVJ-E/H1299; and lane 6, H1299 (A). Clonogenic assay: in the cell line treated with Ku80 siRNA, the surviving fraction of the A549 cells treated with 2-Gy irradiation is reduced by 26%, and the surviving fraction of the H1299 cells is reduced by 14% compared with the untreated cell line. Radiation sensitivity is enhanced by treatment with Ku80 siRNA. All experiments were performed in triplicate. Data are presented as the mean ± SE (B).

HVJ-E or the untransfected cells. We focused on the results of 2-Gy irradiation, which is the usual dose for a single fraction in the clinic. The increased radiation sensitivity at 2-Gy irradiation corresponded to 26 and 14% for Ku80 silencing in the A549 and H1299 cells, respectively.

Radiation sensitivity enhancement by Ku80 siRNA in several human cancer cell lines. After controlling and suppressing Ku80 in tumor cells alternately using siRNA, it was important to verify if radiation sensitivity can be enhanced regardless of the modality and radiation survival rate of a tumor. Another five cancer cell lines, TE13, PCNA-1, MIAPaCa-2, DU-145, and ME-180, were selected for the Ku80 siRNA experiments, because radiation therapy is usually effective for these cancers. Western blot analyses of Ku80 protein expression in all cell

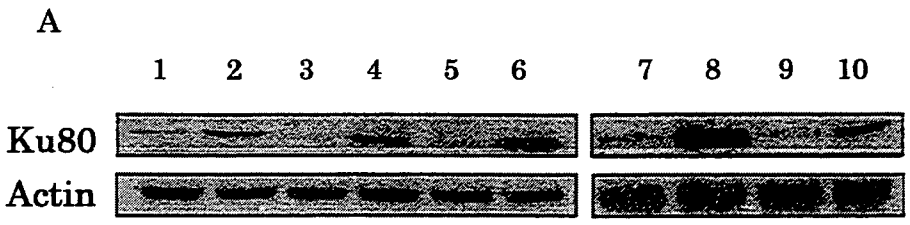

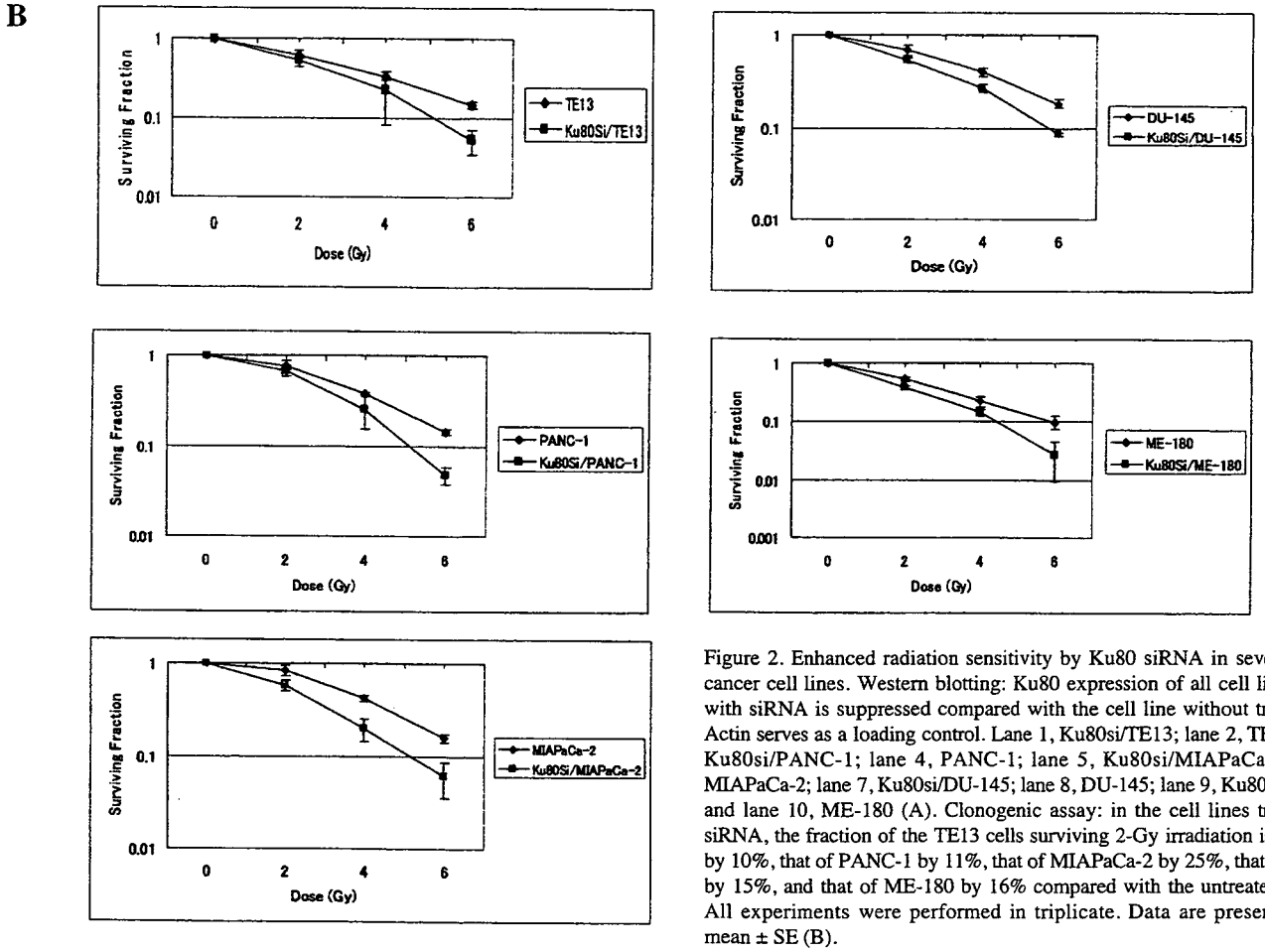

Figure 2. Enhanced radiation sensitivity by Ku80 siRNA in several human cancer cell lines. Western blotting: Ku80 expression of all cell lines treated with siRNA is suppressed compared with the cell line without transfection. Actin serves as a loading control. Lane 1, Ku80si/TE13; lane 2, TE13; lane 3, Ku80si/PANC-1; lane 4, PANC-1; lane 5, Ku80si/MIAPaCa-2; lane 6, MIAPaCa-2; lane 7, Ku80si/DU-145; lane 8, DU-145; lane 9, Ku80si/ME-180; and lane 10, ME-180 (A). Clonogenic assay: in the cell lines treated with siRNA, the fraction of the TE13 cells surviving 2-Gy irradiation is decreased by 10%, that of PANC-1 by 11%, that of MIAPaCa-2 by 25%, that of DU-145 by 15%, and that of ME-180 by 16% compared with the untreated cell line. All experiments were performed in triplicate. Data are presented as the mean ± SE (B).

lines were performed as described previously. After transfection of Ku80 siRNA, Ku80 protein expression was suppressed compared with the untransfected cells (Fig. 2A).

In the cell lines treated with siRNA, surviving fractions of TE13 treated with 2-Gy irradiation decreased by 10% that of PANC-1 by 11%, that of MIAPaCa-2 by 25%, that of DU-145 by 15%, and that of ME-180 by 16% compared with untreated cell lines (Fig. 2B). We observed enhanced radiation sensitivity regardless of the cancer type.

Reduced reparative ability of DSBs resulting from combined radiation and siRNA treatment. Ku80 siRNA apparently enhanced radiation sensitivity in several human cancer cell lines. According to the biologic mechanism, we hypothesized that radiation therapy combined with Ku80 silencing would reduce the DSBs reparative ability. Thus, immunofluorescence detection of gamma-H2AX nuclear foci was performed to detect DSBs.

Gamma-H2AX foci were detected after 2-Gy irradiation in the A549 and H1299 cells. Gamma-H2AX foci stained green; all cells counterstained blue with DAPI for nuclear DNA (data not shown). When >10 gamma-H2AX foci were seen in the cell, it was determined as positive. In both cell lines, positive rates of gamma-H2AX foci immediately increased and decreased over time. The two positive rates with siRNA, at 0.5 h after irradiation in A549 cells and at 6 h in H1299 cells, were significantly higher by 77.6% (95% CI, 70-85; p=0.033) and 76.7% (95% CI, 68-86; p=0.026) compared with no siRNA treatment, 64.1 and 57.5%, respectively (Fig. 3). This suggested that the ability of the DSB repair decreased after radiation and siRNA treatment compared with radiation alone.

Suppression of tumor growth by Ku80 siRNA in H1299 xenograft models. To examine further effects of Ku80 siRNA, we conducted *in vivo* experiments with H1299 xenograft tumors. We used the *in vivo* radiation dose of 4-Gy to simplify ascertaining the effect after treatment.

Before testing the two protocols, we first investigated the post-irradiation effects to estimate the efficiency of Ku80

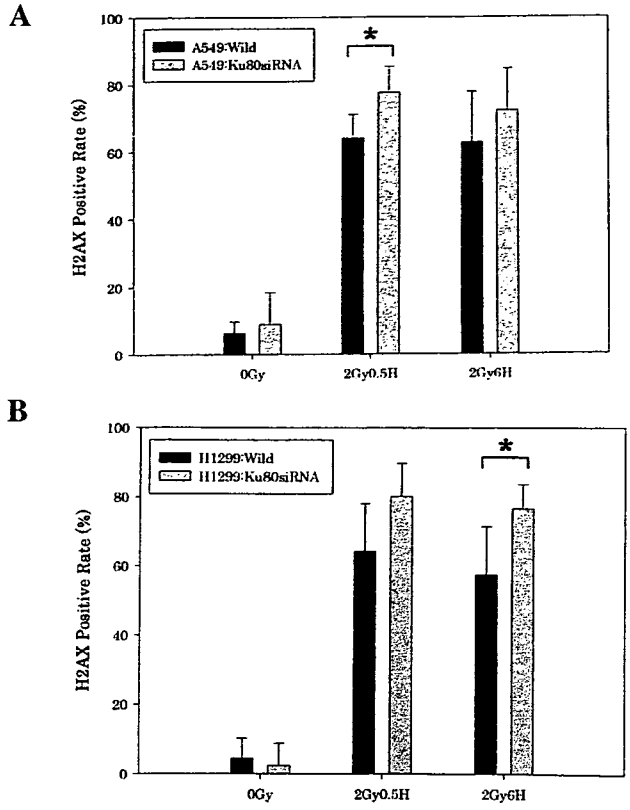

Figure 3. Positive rate of gamma-H2AX foci of A549 and H1299 cells stained 0.5 and 6 h after 2-Gy irradiation. In the A549 cells, the positive rate with siRNA treatment 0.5 h after irradiation is significantly higher than that with no siRNA treatment (p=0.033) (A). In the H1299 cells, the positive rate with siRNA treatment 6 h after irradiation is significantly higher than that with no siRNA treatment (p=0.026). Data are presented as the mean ± SE. H, hours (B).

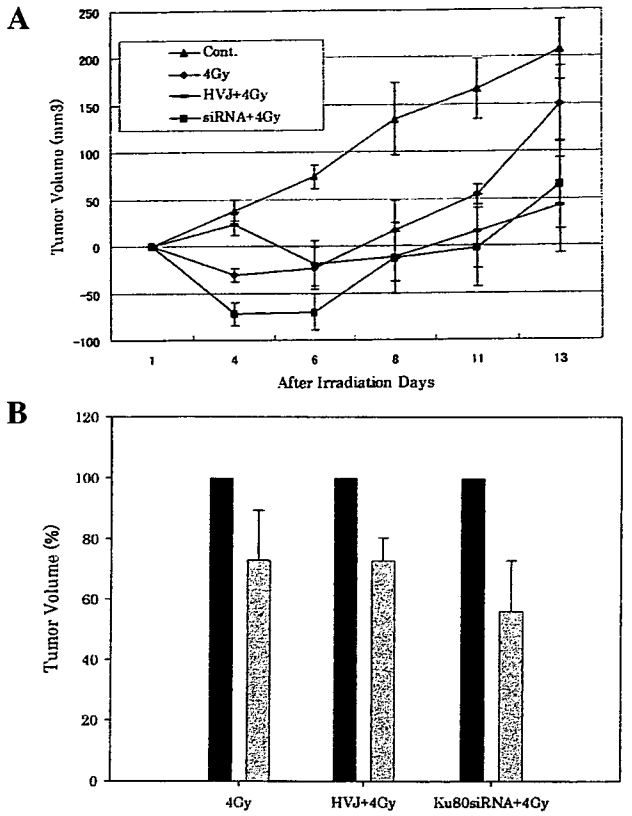

Figure 4. Enhanced tumor growth suppression by Ku80 siRNA combined with radiation therapy. Tumor growth curves for H1299 xenograft tumors treated with irradiation alone, HVJ-E vector, or Ku80 siRNA with irradiation. Quantification of H1299 xenograft increases (>0) or decreases (<0) tumor volumes compared with day 1 (A). The minimum volume of each tumor after irradiation was determined and calculated as a percentage in the various treatment groups compared with day 1 (100%) when the tumor was irradiated. Tumor volumes were measured two or three times weekly. Data are presented as the mean ± SE (B).

siRNA. When tumor volume reached 150-200 mm^3, the mice were randomly divided into four groups: control (n=5), radiation alone (n=4), HVJ-E vector treatment with radiation (n=5), and Ku80 siRNA treatment with radiation (n=6). After 4-Gy radiation, most tumors decreased in volume within 6 days and then began to increase again (Fig. 4A). Fig. 4B shows the percentage of the minimum volumes of each group compared with day 1 (100%). The rate of the reduction in volume of the tumors treated with Ku80 siRNA and radiation was the highest compared with the other groups. The scores of the remaining tumor were 72.95% for radiation alone, 72.70% for HVJ-E with radiation, and 56.02% for Ku80 siRNA with radiation. Even if one treatment was performed, an anti-tumor effect was expected from combination therapy with Ku80 siRNA and irradiation.

Delay in tumor growth by Ku80 siRNA for long-term observation. After confirming the suppression of tumor growth by Ku80 siRNA *in vivo*, the next goal was to follow for a long period the tumors treated with one fraction. When tumor volume reached 150-200 mm^3, the mice were randomly divided into three groups: control (n=11), radiation alone (n=6), and Ku80 siRNA treatment with radiation (n=6). The volume of the tumors in the two groups treated with radiation alone and combination therapy with Ku80 siRNA decreased until day 6 and re-grew in almost parallel fashion (Fig. 5A). By day 32, the increased volume of tumors treated with radiation alone was 404.4±60.2 mm^3 and that of combination therapy with Ku80 siRNA was 308.5±38.2 mm^3, indicating that tumor treated with combination therapy decreased to 76% of the volume of those treated with radiation alone.

The next trial consisted of 5 days of irradiation. To irradiate with five fractions, we waited until the tumor volume reached 750-1000 mm^3, at which point the mice were randomly divided into three groups: control (n=10), radiation alone (n=7), and Ku80 siRNA treatment with radiation (n=8). Irradiation was administered from days 1-5, and Ku80 siRNA was injected into the tumors on days 2 and 4. Until day 15, there was no difference in tumor growth in the two groups, which were treated with radiation alone and combined Ku80 siRNA. After day 15, combination therapy with Ku80 siRNA and radiation resulted in delayed tumor growth (Fig. 5B). By day 32, the increased tumor volume after treatment with five fractions alone was 1476.4±412.5 mm^3 and that of five fractions with two Ku80 siRNA treatments was 830.9±93.8 mm^3, indicating that Ku80 siRNA led to a 56% reduction in volume compared with radiation alone. For example, the proliferation time for the H1299 cell tumor to increase to ~900 mm^3 was

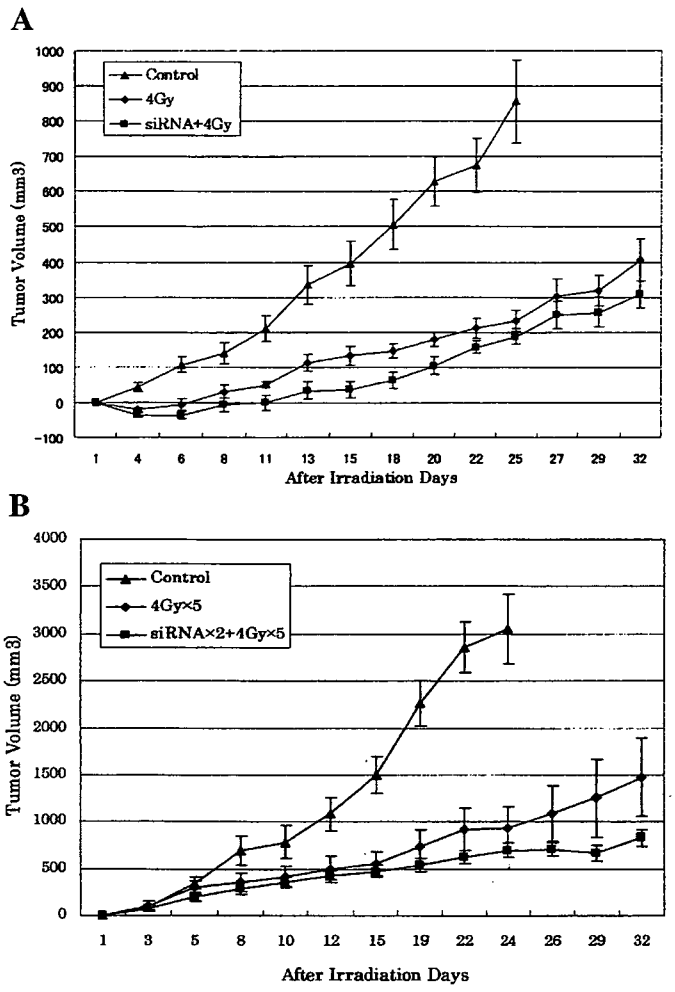

Figure 5. Growth delay curves of H1299 xenograft tumors treated with Ku80 siRNA and long-term irradiation. H1299 xenograft tumors were treated with one Ku80 siRNA treatment on day 0 and one fraction on day 1 (A). Tumors were treated with two Ku80 siRNA treatments on days 2 and 4 and five fractions from days 1 to 5. Data are presented as the mean ± SE (B).

about 22 days for the group treated with radiation alone. However, for the group treated with Ku80 siRNA and radiation, it took >32 days, which indicated a 10-day delay in tumor growth observed after using Ku80 siRNA.

Discussion

Ku80 plays an important role in repairing DNA DSBs, which are common in the DNA damage produced by irradiation (6). Ku was identified as an autoimmune antigen from the sera of a Japanese patient with scleroderma polymyosis overlap syndrome (28). An X-ray-sensitive mutant 5, xrs-5, was isolated from Chinese hamster ovary cell line (CHO K1) which was wild-type of Ku80 and extremely sensitive to irradiation (29). However, after transfection of Ku80 into xrs-5, the cells regained radiation resistance to the same level as CHO K1 (30). Therefore, we focused on Ku80 and hypothesized that silencing Ku80 might enhance radiation sensitivity and be advantageous in treating cancer with irradiation.

In this study, Ku80 protein was suppressed successfully by Ku80 siRNA *in vitro*. Although we chose Ku80 sequences, Ku70 protein expression also was suppressed after transfection with Ku80 siRNA. Loss of one Ku protein was reported to result in a significant decrease in the other Ku protein, because heterodimerization was required to stabilize each Ku protein (29). Furthermore, heterodimerization between Ku70 and Ku80 is essential for DSBs repair and also important in activation of DNA-PKs, which is a main function of Ku80 protein (3). Based on these facts, down-regulation of Ku80 protein by siRNA might have blocked heterodimerization with Ku70, thus inhibiting DNA repair after radiation.

We conducted an additional experiment to prove the inhibition of DNA DSBs repair after using Ku80 siRNA. Immunofluorescence detection of gamma-H2AX nuclear foci is used to detect DNA DSBs. The histone H2AX protein is a variant member of the H2A family of histones that is rapidly phosphorylated at the ser139 residue in response to radiation-induced DNA DSBs, resulting in the formation of nuclear foci (31-33). The prolonged and multiple expressions of H2AX foci after irradiation suggests decreased repair of DNA DSBs (32). Thus, immunofluorescence detection of gamma-H2AX nuclear foci was performed to visualize radiation-induced DSBs after treatment with Ku80 siRNA and to investigate why the radiation sensitivity increased. As expected, combination therapy resulted in enhanced radiation sensitivity. This effect correlated with gamma-H2AX staining, suggesting that the enhanced radiation sensitivity resulted from suppression of the Ku80 protein, which inhibited the ability of the DNA DSBs to repair themselves.

siRNA is expected to be the new therapeutic agent for cancer treatment (9-14). Although various procedures, for example, intravenous and direct injection, are being considered, the important issue is how the anti-tumor effect is acquired efficiently. In the current study, we selected the HVJ-E vector, which has been reported to be a new tool for the transfection reagents and was evaluated as useful and safe *in vitro* and *in vivo* (21-23). We also focused on injecting siRNA included in the HVJ-E vector directly into the tumor *in vivo*. The HVJ-E vector has been extremely safe to handle and efficient for gene transfer, and it might be a powerful candidate for future clinical use.

When cells were transfected with Ku80 siRNA by HVJ-E, Ku80 protein suppression was observed between 18 and 96 h after transfection (data not shown). Thus, we selected 40 h *in vitro* and 20 h *in vivo* after transfection for initiating treatment with radiation therapy to optimize the efficacy. When we used five fractions *in vivo*, we injected siRNA on days 2 and 4, which was 20 h before the radiation on days 3 and day 5. Ito *et al* reported that Rad51 siRNA suppressed protein expression in HeLa cells between 1 and 4 days after transfection and enhanced sensitivity to cisplatin during that period (17). Although each siRNA and cells have their own ability and characteristics, siRNA usually prevents protein expression for a few days; thus, the best timing must be considered for the combination therapy based on efficacy.

In the current study, the cells were treated with one transfection of Ku80 siRNA and one session of irradiation *in vitro*. Even if one treatment was administered, combination therapy with Ku80 siRNA and irradiation obviously enhanced

radiation sensitivity in several types of cancer cell lines. *In vivo*, H1299 xenograft tumors were treated twice with siRNA and five fractions, and the tumor volume decreased compared with radiation alone. However, most patients receive more than 20 fractions in normal clinical practice. So, in the future, we have to establish a regimen close to the clinical protocol, i.e., several treatments with Ku80 siRNA and irradiation.

Since not only malignant tumor cells but also normal tissues are exposed, there are many restrictions in the irradiation procedures, e.g., radiation times and tumor location. If the Ku80 expression in the tumor is inhibited by siRNA and the treatment that enhances radiation sensitivity can be performed for the patients, we may expect improvement in the efficiency of radiation therapy. Furthermore, the indication also may be extended to tumors that have not been targets of radiation therapy.

We showed that Ku80 siRNA included in the HVJ-E vector enhanced the radiation sensitivity of several human cancer cell lines regardless of the cancer type and radiation survival rate *in vitro*. Furthermore, radiation therapy combined with Ku80 siRNA resulted in inhibited tumor growth *in vivo*. Our results indicated that the combination of Ku80 siRNA and irradiation may be a useful novel strategy for cancer treatment considering the biological characteristics.

Acknowledgments

The authors are grateful to Drs Craig W. Stevens and Masaki Takiguchi for support. This study was financially supported by the 21st Century Center of Excellent program at Chiba University, and Grant-in-Aid for Scientific Research on Priority Areas (C) (grant numbers 16591189 and 17591250).

References

1. Haber JE: Partners and pathways repairing a double-strand break. Trends Genet 16: 259-264, 2000.
2. Hoeijmakers JH: Genome maintenance mechanisms for preventing cancer. Nature 411: 366-374, 2001.
3. Jin S and Weaver DT: Double-strand break repair by Ku70 requires heterodimerization with Ku80 and DNA binding functions. EMBO J 16: 6874-6885, 1997.
4. Nick McElhinny SA, Snowden CM, McCarville J and Ramsden DA: Ku recruits the XRCC4-ligase IV complex to DNA ends. Mol Cell Biol 20: 2996-3003, 2000.
5. Bassing CH, Swat W and Alt FW: The mechanism and regulation of chromosomal V(D)J recombination. Cell 109: S45-S55, 2002.
6. Ramsden DA and Gellert M: Ku protein stimulates DNA end joining by mammalian DNA ligases: a direct role for Ku in repair of DNA double-strand breaks. EMBO J 17: 609-614, 1998.
7. Nussenzweig A, Chen C, da Costa Soares V, Sanchez M, Sokol K, Nussenzweig MC and Li GC: Requirement for Ku80 in growth and immunoglobulin V(D)J recombination. Nature 382: 551-555, 1996.
8. Zhu C, Bogue MA, Lim DS, Hasty P and Roth DB: Ku86-deficient mice exhibit severe combined immunodeficiency and defective processing of V(D)J recombination intermediates. Cell 86: 379-389, 1996.
9. Zhang X, Chen ZG, Choe MS, Lin Y, Sun SY, Wieand HS, Shin HJ, Chen A, Khuri FR and Shin DM: Tumor growth inhibition by simultaneously blocking epidermal growth factor receptor and cyclooxygenase-2 in a xenograft model. Clin Cancer Res 11: 6261-6269, 2005.
10. Gao L, Zhang L, Hu J, Li F, Shao Y, Zhao D, Kalvakolanu DV, Kopecko DJ, Zhao X and Xu DQ: Down-regulation of signal transducer and activator of transcription 3 expression using vector-based small interfering RNAs suppresses growth of human prostate tumor *in vivo*. Clin Cancer Res 11: 6333-6341, 2005.
11. Ito T, Hashimoto Y, Tanaka E, Kan T, Tsunoda S, Sato F, Higashiyama M, Okumura T and Shimada Y: An inducible short-hairpin RNA vector against osteopontin reduces metastatic potential of human esophageal squamous cell carcinoma *in vitro* and *in vivo*. Clin Cancer Res 12: 1308-1316, 2006.
12. Halder J, Kamat AA, Landen CN Jr, Han LY, Lutgendorf SK, Lin YG, Merritt WM, Jennings NB, Chavez-Reyes A, Coleman RL, Gershenson DM, Schmandt R, Cole SW, Lopez-Berestein G and Sood AK: Focal adhesion kinase targeting using *in vivo* short interfering RNA delivery in neutral liposomes for ovarian carcinoma therapy. Clin Cancer Res 12: 4916-4924, 2006.
13. Amarzguioui M, Peng Q, Wiiger MT, Vasovic V, Babaie E, Holen T, Nesland JM and Prydz H: *Ex vivo* and *in vivo* delivery of anti-tissue factor short interfering RNA inhibits mouse pulmonary metastasis of B16 melanoma cells. Clin Cancer Res 12: 4055-4061, 2006.
14. Hosaka S, Nakatsura T, Tsukamoto H, Hatayama T, Baba H and Nishimura Y: Synthetic small interfering RNA targeting heat shock protein 105 induces apoptosis of various cancer cells both *in vitro* and *in vivo*. Cancer Sci 97: 623-632, 2006.
15. Peng Y, Zhang Q, Nagasawa H, Okayasu R, Liber HL and Bedford JS: Silencing expression of the catalytic subunit of DNA-dependent protein kinase by small interfering RNA sensitizes human cells for radiation-induced chromosome damage, cell killing, and mutation. Cancer Res 62: 6400-6404, 2002.
16. Collis SJ, Swartz MJ, Nelson WG and De Weese TL: Enhanced radiation and chemotherapy-mediated cell killing of human cancer cells by small inhibitory RNA silencing of DNA repair factors. Cancer Res 63: 1550-1554, 2003.
17. Ito M, Yamamoto S, Nimura K, Hiraoka K, Tamai K and Kaneda Y: Rad51 siRNA delivered by HVJ envelope vector enhances the anti-cancer effect of cisplatin. J Gene Med 7: 1044-1052, 2005.
18. Zhang Y, Lim CUK, Williams ES, Zhou J, Zhang Q, Fox MH, Bailey SM and Liber HL: *NBS1* knockdown by small interfering RNA increases ionizing radiation mutagenesis and telomere association in human cells. Cancer Res 65: 5544-5553, 2005.
19. Ohnishi K, Scuric Z, Schiestl RH, Okamoto N, Takahashi A and Ohnishi T: siRNA targeting *NBS1* or *XIAP* increases radiation sensitivity of human cancer cells independent of *TP53* satus. Radiat Res 166: 454-462, 2006.
20. Xu M, Myerson RJ, Hunt C, Kumar S, Moros EG, Straube WL and Roti JL: Transfection of human tumor cells with Mre11 siRNA and the increase in radiation sensitivity and the reduction in heat-induced radiosensitization. Int J Hyperthermia 20: 157-162, 2004.
21. Kaneda Y, Nakajima T, Nishikawa T, Yamamoto S, Ikegami H, Suzuki N, Nakamura H, Morishita R and Kotani H: Hemagglutinating virus of Japan (HVJ) envelope vector as a versatile gene delivery system. Mol Ther 6: 219-226, 2002.
22. Shimamura M, Morishita R, Endoh M, Oshima K, Aoki M, Waguri S, Uchiyama Y and Kaneda Y: HVJ-envelope vector for gene transfer into central nervous system. Biochem Biophys Res Commun 300: 464-471, 2003.
23. Nakamura H, Kimura T, Ikegami H, Ogita K, Koyama S, Shimoya K, Tsujie T, Koyama M, Kaneda Y and Murata Y: Highly efficient and minimally invasive *in vivo* gene transfer to the mouse uterus using haemagglutinating virus of Japan (HVJ) envelope vector. Mol Hum Reprod 9: 603-609, 2003.
24. Kojima C, Hashimoto A, Yabuta I, Hirose M, Hashimoto S, Kanaho Y, Sumimoto H, Ikegami T and Sabe H: Regulation of Bin1 SH3 domain binding by phosphoinositides. EMBO J 23: 4413-4422, 2004.
25. Ohnuma K, Yamochi T, Uchiyama M, Nishibashi K, Yoshikawa N, Shimizu N, Iwata S, Tanaka H, Dang NH and Morimoto C: CD26 up-regulates expression of CD86 on antigen-presenting cells by means of caveolin-1. Proc Natl Acad Sci USA 101: 14186-14191, 2004.
26. Sumi K, Yokozeki H, Wu MH, Satoh T, Kaneda Y, Takeda K, Akira S and Nishioka K: *In vivo* transfection of a cis element 'decoy' against signal transducers and activators of the transcription 6 (STAT6) binding site ameliorates the response of contact hypersensitivity. Gene Ther 11: 1763-1771, 2004.
27. Nimura Y, Ismail SM, Kurimas A, Chen DJ and Stevens CW: DNA-PK and ATM are required for radiation-enhanced integration. Radiat Res 157: 562-567, 2002.

28. Mimori T, Akizuki M, Yamagata H, Inada S, Yoshida S and Homma M: Characterization of a high molecular weight acidic nuclear protein recognized by autoantibodies in sera from patients with polymyositis-scleroderma overlap. J Clin Invest 68: 611-620, 1981.
29. Singleton BK, Priestley A, Steingrimsdottir H, Gell D, Blunt T, Jackson SP, Lehmann AR and Jeggo PA: Molecular and biochemical characterization of xrs mutants defective in Ku80. Mol Cell Biol 17: 1264-1273, 1997.
30. Stevens CW, Stamato TD, Mauldin SK, Getts RC, Zeng M and Cerniglia GJ: Radiation-induced recombination is dependent on Ku80. Radiat Res 151: 408-413, 1999.
31. Rogakou EP, Boon C, Redon C and Bonner WM: Megabase chromatin domains involved in DNA double strand breaks *in vivo*. J Cell Biol 146: 905-916, 1999.
32. Rothkamm K, Krüger I, Thompson LH and Lobrich M: Pathways of DNA double-strand break repair during the mammalian cell cycle. Mol Cell Biol 23: 5706-5715, 2003.
33. Camphausen K, Burgan W, Cerra M, Oswald KA, Trepel JB, Lee MJ and Tofilon PJ: Enhanced radiation-induced cell killing and prolongation of γ-H2AX foci expression by the histone deacetylase inhibitor MS-275. Cancer Res 64: 316-321, 2004.

Oncogene (2007) 26, 5669–5673

www.nature.com/onc

SHORT COMMUNICATION

DFF45/ICAD restores cisplatin-induced nuclear fragmentation but not DNA cleavage in *DFF45*-deficient neuroblastoma cells

M Takahashi[1,2], T Ozaki[1], A Takahashi[1,3], M Miyauchi[4], S Ono[3], N Takada[1,2], T Koda[3], S Todo[2], T Kamijo[1] and A Nakagawara[1]

[1]Division of Biochemistry, Chiba Cancer Center Research Institute, Chuoh-ku, Chiba, Japan; [2]Department of General Surgery, Hokkaido University School of Medicine, Kita-ku, Sapporo, Japan; [3]Center for Functional Genomics, Hisamitsu Pharmaceutical Co., Inc., Chuoh-ku, Chiba, Japan and [4]Division of Pathology, Chiba Cancer Center Research Institute, Chuoh-ku, Chiba, Japan

We have previously defined a homozygously deleted region at chromosome 1p36.2–p36.3 in human neuroblastoma cell lines, NB-1 and NB-C201, and identified six genes including *DFF45/ICAD* within this region. In this study, we found that NB-C201 cells are much more resistant to various genotoxic stresses such as cisplatin (CDDP) than CHP134 and SH-SY5Y cells that do not have the homozygous deletion. To examine a role(s) of DFF45 in the regulation of apoptosis in response to CDDP, we have established stably DFF45-expressing NB-C201 cell clones (DFF45-1 and DFF45-3) and a control cell clone (NB-C201-C) using a retrovirus-mediated gene transfer. In contrast to NB-C201-C cells, DFF45-3 cells displayed apoptotic nuclear fragmentation in response to CDDP. Although CDDP-induced proteolytic cleavage of procaspase-3 and DFF45 in DFF45-3 cells, we could not detect a typical apoptotic DNA fragmentation. Additionally, deletion analysis revealed that C-terminal region of DFF45 is required for inducing nuclear fragmentation. Unexpectedly, (3-(4,5-dimethylthiazol-2-yl)-2,5-diphenyltetrazolium bromide (MTT) assays demonstrated that DFF45 has undetectable effect on CDDP sensitivity of NB-C201 cells. Taken together, our present results suggest that DFF45/DFF40 system may be sufficient for CDDP-induced nuclear fragmentation but not DNA cleavage.

Oncogene (2007) **26**, 5669–5673; doi:10.1038/sj.onc.1210352; published online 12 March 2007

Keywords: apoptosis; cisplatin; DFF45/ICAD; homozygous deletion; neuroblastoma

Neuroblastoma (NBL) is one of the most common pediatric solid tumors and displays various clinical behaviors (Brodeur and Nakagawara, 1992). Loss at the distal part of the short arm of chromosome 1 (1p) and the amplification of *MYCN* in NBL are strongly associated with an unfavorable prognosis (Brodeur *et al.*, 1984). Extensive loss of heterozygosity (LOH) analysis narrowed the overlapping deleted region of 1p in NBL, suggesting that there could be at least three NBL suppressor loci (Schleiermacher *et al.*, 1994; Takeda *et al.*, 1994; Amler *et al.*, 1995; Cheng *et al.*, 1995; Martinsson *et al.*, 1995; White *et al.*, 1995). We found that NBL cell lines, NB-1 and NB-C201, carry a homozygous deletion at 1p36.2, and identified six genes within this region including *DFF45/ICAD*, *PGD*, *CORT*, *UFD2a*, *KIF1B-β* and *PEX14* (Ohira *et al.*, 2000). Among them, we have demonstrated that UFD2a promotes the proteasome-dependent degradation of p73 (Hosoda *et al.*, 2005).

Apoptosis is defined by a series of morphological and biochemical changes. DNA fragmentation is one of characteristic features of apoptosis (Raff, 1992) and triggered by a heterodimeric DNA fragmentation factor (DFF), which is composed of DFF40/CAD/CPAN nuclease and its inhibitor DFF45/ICAD. Upon apoptotic stimuli, DFF45 is cleaved by caspase-3 into three fragments and dissociates from DFF40, resulting in the activation of DFF40 (Liu *et al.*, 1997, 1998; Enari *et al.*, 1998; Halenbeck *et al.*, 1998; Mukae *et al.*, 1998; Sakahira *et al.*, 1998). DFF45 also acts as a folding chaperone required to produce active DFF40 (Enari *et al.*, 1998; Sakahira *et al.*, 1998). In this study, we examined a role(s) of DFF45 in the regulation of NBL cell death.

To assess the biological significance of the above-mentioned six genes, we compared the drug sensitivity of NBL cells with or without the homozygous deletion. NB-C201, CHP134 and SH-SY5Y cells were exposed to various genotoxic agents including cisplatin (CDDP), adriamycin (ADR) or etoposide (VP16), and their viability was monitored by (3-(4,5-dimethylthiazol-2-yl)-2,5-diphenyltetrazolium bromide (MTT) assay. As shown in Figure 1a, NB-C201 cells were much more resistant to CDDP, ADR and VP16 compared with CHP134 and SH-SY5Y cells. In accordance with these results, NB-C201 cells showed chromatin condensation in response to CDDP; however, nuclear fragmentation, which is one of morphological hallmarks of apoptosis (Wyllie, 1980), was undetectable in NB-C201 cells exposed to CDDP (Figure 1b). As DFF45-deficient cells showed a decreased

Correspondence: Dr A Nakagawara, Division of Biochemistry, Chiba Cancer Center Research Institute, 666-2 Nitona, Chuoh-ku, Chiba 260-8717, Japan.
E-mail: akiranak@chiba-cc.jp
Received 17 July 2006; revised 22 January 2007; accepted 23 January 2007; published online 12 March 2007

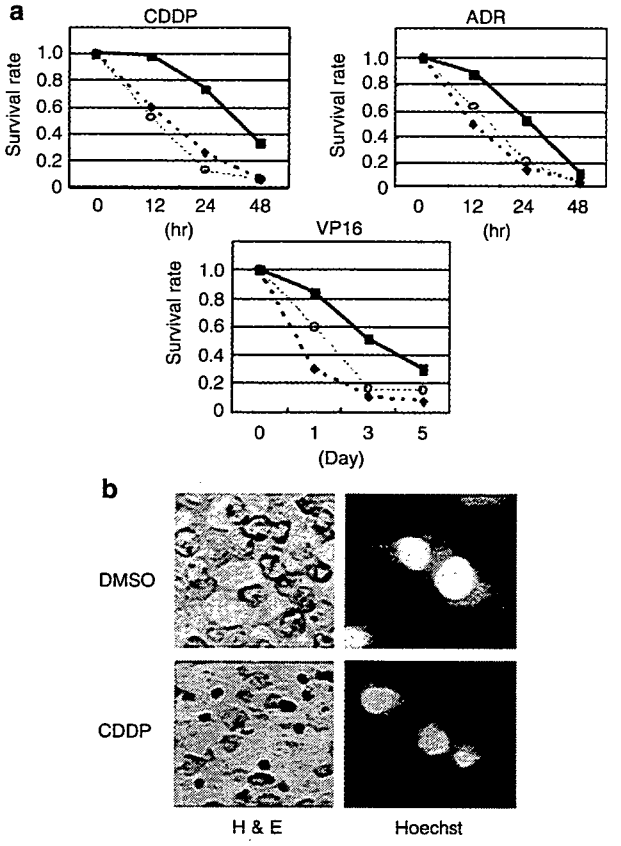

Figure 1 CDDP sensitivity of *DFF45*-deficient NBL cell. (**a**) Effect of various genotoxic agents on NBL cells. NB-C201 (■), CHP134 (♦) and SH-SY5Y (□) cells were treated with CDDP (25 μM), ADR (1 μg/ml) or VP16 (50 μM). At the indicated time periods, cell viability was determined by MTT assays. Data are shown as the number of viable cells relative to that of untreated cells, which is arbitrarily assigned a value of 1.0. (**b**) Chromatin condensation of CDDP-treated NB-C201 cells. NB-C201 cells were exposed to DMSO (top panels) or 25 μM of CDDP (bottom panels) for 24 h. Cells were processed for hematoxylin and eosin (H&E) staining (left panels) or stained with Hoechst dye to reveal the degree of chromatin condensation (right panels).

sensitivity to apoptotic stimuli (Zhang *et al.*, 1999), we tested a possibility that the lack of DFF45 is responsible for the drug resistance of NBL cells. We first examined the expression of *DFF45* and *DFF40* in various NBL cell lines by Northern blot analysis. HeLa cells were used as a positive control (Liu *et al.*, 1997). As reported (Ohira *et al.*, 2000), *DFF45* was undetectable in NB-1 and NB-C201 cells, whereas variable levels of *DFF45* were detected in the remaining cells (Figure 2a, top panel). Previous results indicated that *DFF45* is expressed as two transcripts of 3.8 and 2.4 kb in length (Zhang *et al.*, 1999). However, Yang *et al.* (2001) described that some different-sized mRNAs are expressed in several NBL cell lines. We observed four *DFF45* transcripts of 5.4, 3.8, 2.4 and 1.6 kb in length. On the other hand, a single *DFF40* transcript (3.4 kb) was detectable in all NBL cell lines (Figure 2a, middle panel) as reported in other cell types (Mukae *et al.*, 1998). Immunoblot analysis also revealed that substantial amounts of DFF45 and DFF40 are expressed in SH-SY5Y and CHP134 cells, whereas NB-C201 cells express DFF40 but not DFF45 (Figure 2b).

To explore the role of DFF45 in response to CDDP, the retroviral vector encoding DFF45 was introduced into NB-C201 cells and stable cell clones were established. As shown in Figure 2c, DFF45-1, -3, -4, -7, and -8 clones expressed relatively larger amounts of DFF45 compared with the remaining clones. DFF45 was not detectable in NB-C201 cells infected with an empty vector (NB-C201-C). The enforced expression of DFF45 did not affect the expression levels of DFF40 (Figure 2d). We employed DFF45-1 and DFF45-3 cells for further experiments. Consistent with the previous observations (Liu *et al.*, 1998), exogenously expressed DFF45 was largely localized in cell nucleus (Figure 2e). We then examined whether DFF45 could affect CDDP sensitivity of NB-C201 cells. NB-C201-C, DFF45-1 and DFF45-3 cells were treated with CDDP for the indicated time periods and their viability was measured by the MTT assay. Unexpectedly, DFF45 had no detectable effects on the viability of NB-C201 cells in response to CDDP (Figure 2f).

We then addressed whether DFF45 could affect the nuclear morphology in response to CDDP. NB-C201-C and DFF45-3 cells were exposed to CDDP for 48 h and their nuclear morphology was examined. As seen in Figure 3a, Hoechst staining clearly demonstrated that apoptotic nuclear fragmentation takes place in DFF45-3 cells, but not in NB-C201-C cells. These results were confirmed by electron microscopic analysis (Figure 3b). Similar results were also obtained in DFF45-1 cells (data not shown). We sought to examine whether DFF45 could promote DNA fragmentation in response to CDDP by TUNEL staining. CDDP-sensitive CHP134 cells were used as a positive control. Unexpectedly, we observed no TUNEL-positive nuclei in DFF45-3 cells (Figure 3c). DNA fragmentation as assessed by agarose gel electrophoresis did not occur in DFF45-3 cells exposed to CDDP. As described previously (Enari *et al.*, 1998; Liu *et al.*, 1998), caspase-3-dependent cleavage of DFF45 was required for the activity of DFF40. We therefore addressed a possibility that caspase-3-mediated cleavage of DFF45 could be impaired owing to a loss of the activation of caspase-3 in DFF45-3 cells in response to CDDP. As shown in Figure 3e, the time-dependent cleavage of procaspase-3 and DFF45 was observed in DFF45-3 cells. Thus, DFF45 induced nuclear fragmentation, but not DNA fragmentation in NB-C201 cells.

We then examined whether the region(s) of DFF45 involved in nuclear fragmentation could be distinct from that required for DNase activity. To this end, we constructed a series of FLAG-tagged DFF45 deletion mutants (Figure 4a) and then introduced them into NB-C201 cells. After 2 weeks of culture in the presence of G418, drug-resistant colonies were combined and expanded. As shown in Figure 4b, each vector gave rise to a stable protein with the expected size. CDDP-induced nuclear fragmentation in NB-C201 cells expressing wild-type DFF45, whereas DFF45 (1–290), DFF45 (1–231) or

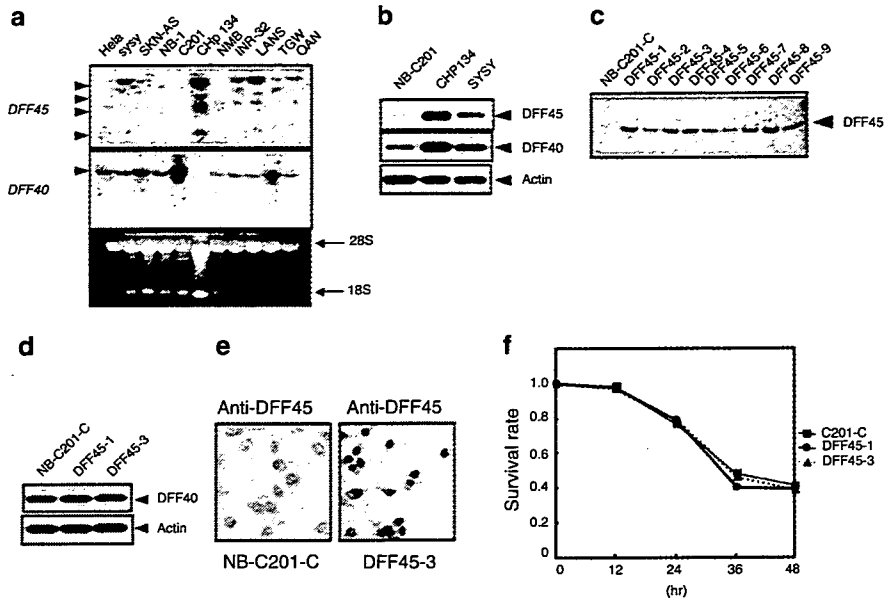

Figure 2 Enforced expression of DFF45 in NB-C201 cells. (**a**) Expression of *DFF45* and *DFF40* in various NBL cell lines. Total RNA from the indicated cells was subjected to Northern blot analysis using the radiolabeled *DFF45* (top panel) or *DFF40* (middle panel) cDNA. Relative RNA loading is indicated by the intensity of the 18S and 28S rRNA bands (bottom panel). (**b**) Expression of DFF45 and DFF40 in NBL cells. Lysates from the indicated cells were processed for immunoblotting with anti-DFF45 (top panel) or anti-DFF40 (middle panel) antibody. (**c**) Immunoblot analysis. Lysates from the indicated cell clones were subjected to immunoblotting with anti-DFF45 antibody. (**d**) Expression of DFF40 in stable cell clones. Lysates from the indicated cell clones were subjected to immunoblotting with anti-DFF40 antibody. (**e**) Immunostaining. Four-micrometer sections of paraffin-embedded, formaldehyde-fixed NB-C201-C (left panel) and DFF45-3 (right panel) cells were deparaffinized in xylene, rehydrated through a series of ethanol and then stained with anti-DFF45 antibody. (**f**) Effects of DFF45 on CDDP sensitivity. NB-C201-C (■), DFF45-1 (•) and DFF45-3 (▲) cells were treated with 25 μM of CDDP. At the indicated time periods, cell viability was measured by MTT assays.

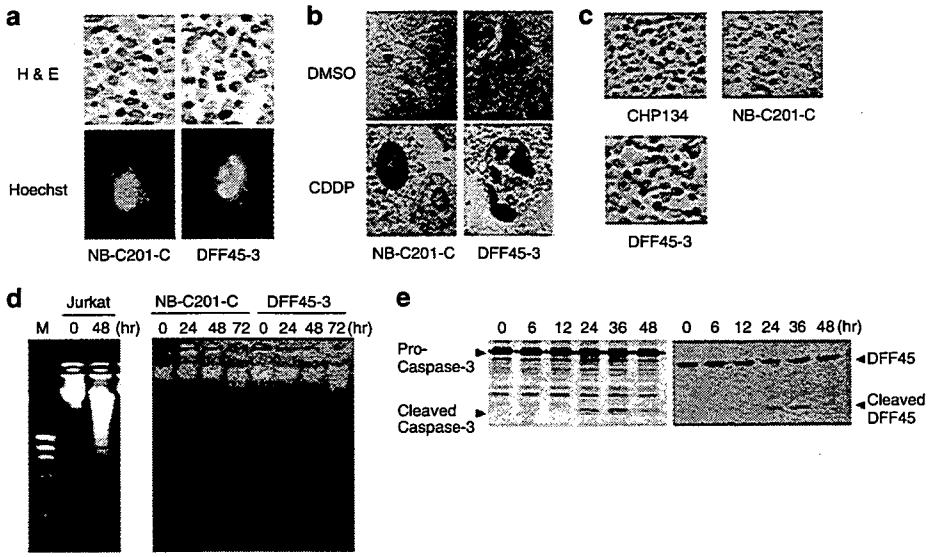

Figure 3 DFF45 promotes nuclear fragmentation but not DNA fragmentation. (**a**) Nuclear fragmentation of CDDP-treated DFF45-3 cells. NB-C201-C (left panels) and DFF45-3 (right panels) cells were exposed to 25 μM of CDDP. Forty-eight hours after treatment, cells were stained with H&E (top panels) or with Hoechst dye (bottom panels). (**b**) Electron micrographs. NB-C201-C (left panels) and DFF45-3 (right panels) cells were exposed to 25 μM of CDDP (bottom panels) or left untreated (top panels). Forty-eight hours after CDDP treatment, NB-C201-C and DFF45-3 cells were fixed, embedded with an epoxy resin, and grid-mounted sections were then processed for transmission electron microscopy. (**c**) TUNEL staining. CHP134, NB-C201-C and DFF45-3 cells were treated with 25 μM of CDDP. Forty-eight hours after CDDP treatment, cells were stained for TUNEL (Roche Applied Science, Indianapolis, IN, USA). (**d**) DNA fragmentation assay. Jurkat, NB-C201-C and DFF45-3 cells treated with CDDP (25 μM) for the indicated time periods were used for genomic DNA preparation. After RNase A treatment, genomic DNA was subjected to 1.5% agarose gel electrophoresis and visualized under ultraviolet light. (**e**) Caspase-3 activation in response to CDDP. DFF45-3 cells were exposed to 25 μM of CDDP. At the indicated time points after the drug exposure, lysates were subjected to immunoblotting with anti-caspase-3 (Pharmingen, San Jose, CA, USA) (left panel) or anti-DFF45 (C-19; Santa Cruz Biotechnology, Santa Cruz, CA, USA) (right panel) antibody.

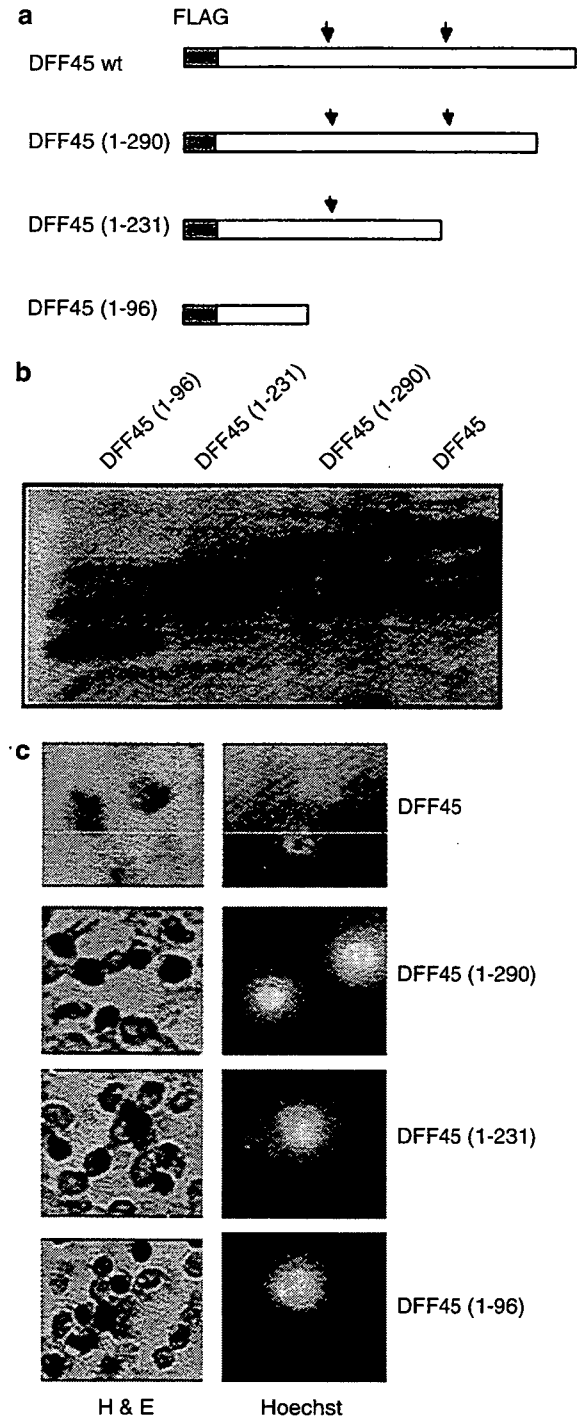

Figure 4 C-terminal region of DFF45 is required for CDDP-induced nuclear fragmentation. (**a**) Schematic representation of a series of FLAG-tagged deletion mutants of DFF45. Closed arrowheads indicate the positions of caspase-3 cleavage sites. (**b**) Expression of DFF45 deletion mutants. Lysates from NB-C201 cells infected with the indicated retroviral vector were subjected to immunoblotting with anti-FLAG (M2; Sigma, St Louis, MO, USA) antibody. (**c**) Effect of DFF45 deletion mutants on nuclear morphology in the presence of CDDP. NB-C201 cells infected with the indicated retroviral vector were exposed to CDDP (25 μM) for 48 h. Cells were then stained with H&E (left panels) or with Hoechst dye to reveal the degree of nuclear fragmentation (right panels).

DFF45 (1–96) failed to induce nuclear fragmentation in response to CDDP (Figure 4c), suggesting that COOH-terminal region of DFF45 is essential for the induction of nuclear fragmentation in NB-C201 cells. As described by Gu *et al.* (1999), central domain of DFF45 (amino-acid residues 101–180) is required for the interaction with DFF40 and DFF45 can assist in the synthesis of highly active DFF40. In addition, the catalytic domain of DFF40 is located in its COOH-terminal region (amino-acid residues 290–345) (Inohara *et al.*, 1999). As our mutation searches revealed that NB-C201 cells express wild-type *DFF40* (data not shown), it is likely that CDDP-mediated nuclear fragmentation might be regulated in a DFF45- but not in a DFF40-dependent manner.

As described by Ohira *et al.* (2000), we failed to detect any mutations within *DFF45* in NBLs. Similar results were reported by Yang *et al.* (2001). In this study, we found that DFF45 can selectively restore the ability to induce nuclear fragmentation but not DNA cleavage in response to CDDP. Recently, it has been shown that γH2AX regulates DNA fragmentation mediated by DFF40 (Lu *et al.*, 2006). Our preliminary experiments revealed that the amounts of γH2AX remain unchanged regardless of CDDP treatment (data not shown). Moreover, chromatin condensation and nuclear fragmentation have been shown to be regulated by nucleoplasmin, indicating that nuclear morphological changes and DNA fragmentation are independent processes (Lu *et al.*, 2005). Further efforts should be devoted to delineate whether such dissociation of nucleolytic and DNase activities of DFF45/DFF40 system in a subset of NBL cells contributes to the highly variable clinical behavior of this neoplasm.

Acknowledgements

This work was supported in part by a Grant-in-Aid from the Ministry of Health, Labour and Welfare for Third Term Comprehensive Control Research for Cancer, and a Grant-in-Aid for Cancer Research from the Ministry of Health, Labour and Welfare of Japan, a Grant-in-Aid for Scientific Research on Priority Areas from the Ministry of Education, Culture, Sports, Science and Technology, Japan, and a grant from Uehara Memorial Foundation.

References

Amler LC, Corvi R, Praml C, Savelyeva L, Le Paslier D, Schwab M. (1995). A reciprocal translocation (1;15)(36.2;q24) in a neuroblastoma cell line is accompanied by DNA duplication and may signal the site of a putative tumor suppressor gene. *Oncogene* **10**: 1095–1101.

Brodeur GM, Seeger RC, Schwab M, Varmas HE, Bishop JM. (1984). Amplification of N-*myc* in untreated human neuroblastomas corelates with advanced disease stage. *Science* **224**: 1121–1124.

Brodeur GM, Nakagawara A. (1992). Molecular basis of clinical heterogeneity in neuroblastoma. *Am J Pediatr Hematol Oncol* **14**: 111–116.

Cheng NC, Van Roy N, Chan A, Beitsma M, Westerveld A, Speleman F *et al.* (1995). Deletion mapping in neuroblastoma cell lines suggests two distinct tumor suppressor genes

in the 1p35–36 region, only one of which is associated with N-myc amplification. *Oncogene* **10**: 291–297.

Enari M, Sakahira H, Yokoyama H, Okawa K, Iwamatsu A, Nagata S. (1998). A caspase-activated DNase that degrades DNA during apoptosis, and its inhibitor ICAD. *Nature* **391**: 43–50.

Gu J, Dong RP, Zhang C, McLaughlin DF, Wu MX, Schlossman SF. (1999). Functional interaction of DFF35 and DFF45 with caspase-activated DNA fragmentation nuclease DFF40. *J Biol Chem* **274**: 20759–20762.

Halenbeck R, MacDonald H, Roulston A, Chen TT, Conroy L, Williams LT. (1998). CPAN, a human nuclease regulated by the caspase-sensitive inhibitor DFF45. *Curr Biol* **8**: 537–540.

Hosoda M, Ozaki T, Miyazaki K, Hayashi S, Furuya S, Watanabe K *et al.* (2005). UFD2a mediates the proteasomal turnover of p73 without promoting p73 ubiquitination. *Oncogene* **24**: 7156–7169.

Inohara N, Koseki T, Chen S, Benedict MA, Nunez G. (1999). Identification of regulatory and catalytic domains in the apoptosis nuclease DFF40/CAD. *J Biol Chem* **274**: 270–274.

Liu X, Zou H, Slaughter C, Wang X. (1997). DFF, a heterodimeric protein that functions downstream of caspase-3 to trigger DNA fragmentation during apoptosis. *Cell* **89**: 175–184.

Liu X, Li P, Widlak P, Zou H, Luo X, Garrard WT *et al.* (1998). The 40-kDa subunit of DNA fragmentation factor induces DNA fragmentation and chromatin condensation during apoptosis. *Proc Natl Acad Sci USA* **95**: 8461–8466.

Lu C, Zhu F, Cho YY, Tang F, Zykova T, Ma WY *et al.* (2006). Cell apoptosis: requirement of H2AX in DNA ladder formation, but not for the activation of caspase-3. *Mol Cell* **23**: 121–132.

Lu Z, Zhang C, Zhai Z. (2005). Nucleoplasmin regulates chromatin condensation during apoptosis. *Proc Natl Acad Sci USA* **102**: 2778–2783.

Martinsson T, Sjoberg RM, Hedborg F, Kogner P. (1995). Deletion of chromosome 1p loci and microsatellite instability in neuroblastomas analyzed with short-tandem repeat polymorphisms. *Cancer Res* **55**: 5681–5686.

Mukae N, Enari M, Sakahira H, Fukuda Y, Inazawa J, Tho H *et al.* (1998). Molecular cloning and characterization of human caspase- activated DNase. *Proc Natl Acad Sci USA* **95**: 9123–9128.

Ohira M, Kageyama H, Mihara M, Furuta S, Machida T, Shishikura T *et al.* (2000). Identification and characterization of a 500-kb homozygously deleted region at 1p36.2–p36.3 in a neuroblastoma cell line. *Oncogene* **19**: 4302–4307.

Raff MC. (1992). Social controls on cell survival and cell death. *Nature* **356**: 397–400.

Sakahira H, Enari M, Nagata S. (1998). Cleavage of CAD inhibitor in CAD activation and DNA degradation during apoptosis. *Nature* **391**: 96–99.

Schleiermacher G, Peter M, Michon J, Hugot JP, Vielh P, Zucker JM *et al.* (1994). Two distinct deleted regions on the short arm of chromosome 1 in neuroblastoma. *Genes Chromosomes Cancer* **10**: 275–281.

Takeda O, Homma C, Maseki N, Sakurai M, Kanda N, Schwab M *et al.* (1994). There may be two tumor suppressor genes on chromosome arm 1p closely associated with biologically distinct subtypes of neuroblastoma. *Genes Chromosomes Cancer* **10**: 30–39.

White PS, Maris JM, Beltinger C, Sulman E, Marshall HN, Fujimori M *et al.* (1995). A region of consistent deletion in neuroblastoma maps within human chromosome 1p36.2–36.3. *Proc Natl Acad Sci USA* **92**: 5520–5524.

Wyllie AH. (1980). Glucocorticoid-induced thymocyte apoptosis is associated with endogenous endonuclease activation. *Nature* **284**: 555–556.

Yang HW, Chen YZ, Piao HY, Takita J, Soeda E, Hayashi Y. (2001). DNA fragmentation factor 45 (DFF45) gene at 1p36.2 is homozygously deleted and encodes variant transcripts in neuroblastoma cell line. *Neoplasia* **3**: 165–169.

Zhang J, Wang X, Bove KE, Xu M. (1999). DNA fragmentation factor 45-deficient cells are more resistant to apoptosis and exhibit different dying morphology than wild-type control cells. *J Biol Chem* **274**: 37450–37454.

THE JOURNAL OF BIOLOGICAL CHEMISTRY VOL. 282, NO. 25, pp. 18365–18378, June 22, 2007

Stabilization of p73 by Nuclear IκB Kinase-α Mediates Cisplatin-induced Apoptosis*

Received for publication, November 13, 2006, and in revised form, April 23, 2007 Published, JBC Papers in Press, April 23, 2007, DOI 10.1074/jbc.M610522200

Kazushige Furuya[‡§], Toshinori Ozaki[‡], Takayuki Hanamoto[‡], Mitsuchika Hosoda[‡], Syunji Hayashi[‡], Philip A. Barker[¶], Kunio Takano[§], Masahiko Matsumoto[§], and Akira Nakagawara[‡1]

From the [‡]Division of Biochemistry, Chiba Cancer Center Research Institute, Chiba 260-8717, Japan, the [§]Second Department of Surgery, Yamanashi University School of Medicine, Yamanashi 409-3898, Japan, and the [¶]Montreal Neurological Institute, McGill University, Montreal, Quebec H3A 2B4, Canada

In response to DNA damage, p53 and its homolog p73 have a function antagonistic to NF-κB in deciding cell fate. Here, we show for the first time that p73, but not p53, is stabilized by physical interaction with nuclear IκB kinase (IKK)-α to enhance cisplatin (CDDP)-induced apoptosis. CDDP caused a significant increase in the amounts of nuclear IKK-α and p73α in human osteosarcoma-derived U2OS cells. Ectopic expression of IKK-α prolonged the half-life of p73 by inhibiting its ubiquitination and thereby enhancing its transactivation and pro-apoptotic activities. Consistent with these results, small interfering RNA-mediated knockdown of endogenous IKK-α inhibited the CDDP-mediated accumulation of p73α. The kinase-deficient mutant form of IKK-α interacted with p73α, but failed to stabilize it. Furthermore, CDDP-mediated accumulation of endogenous p73α was not detected in mouse embryonic fibroblasts (MEFs) prepared from IKK-α-deficient mice, and CDDP sensitivity was significantly decreased in IKK-α-deficient MEFs compared with wild-type MEFs. Thus, our results strongly suggest that the nuclear IKK-α-mediated accumulation of p73α is one of the novel molecular mechanisms to induce apoptotic cell death in response to CDDP, which may be particularly important in killing tumor cells with *p53* mutation.

The NF-κB signaling pathway is activated by a variety of structurally and functionally unrelated stimuli, including inflammatory cytokines, ionizing radiation, viral and bacterial infection, and oxidative stress (reviewed in Refs. 1 and 2). Under normal conditions, NF-κB exists as heterodimeric complexes composed of p50 and p65 (RelA) subunits and is kept transcriptionally inactive through interaction with its inhibitory proteins such as IκB-α and IκB-β. IκB proteins mask the nuclear localization signal of NF-κB, thereby preventing its nuclear translocation. Upon certain stimulations, IκB proteins are rapidly phosphorylated at specific serine residues in the N-terminal their signal-responsive domain by upstream regulator IκB kinase (IKK)[2] complex and subsequently polyubiquitinated and degraded in a proteasome-dependent manner (reviewed in Ref. 3). The high molecular mass IKK complex comprises two related catalytic subunits, IKK-α (also called IKK-1) and IKK-β (also called IKK-2), and one regulatory subunit with a scaffold function, IKK-γ (also called NEMO) (reviewed in Ref. 3). The proteolytic degradation of IκB proteins exposes the nuclear localization signal of NF-κB and results in translocation of NF-κB from the cytoplasm to the nucleus, allowing it to participate in transcriptional regulation of numerous target genes involved in immune responses, inflammatory reactions, cell adhesion, cell proliferation, apoptotic cell death, and other cellular processes. Therefore, the IKK complex represents one of the critical upstream regulators of the NF-κB signaling pathway.

In many experimental systems, the activation of NF-κB has been shown to play an important role in the control of survival processes, protecting cells from a variety of apoptotic signals (4–8). For example, tumor necrosis factor-α (TNF-α) simultaneously activates the NF-κB-mediated cellular protective mechanism against the pro-apoptotic effect of TNF-α through the induction of the NF-κB-responsive genes that function to block apoptosis. Additionally, inhibition of NF-κB has been shown to enhance sensitivity to chemotherapeutic agents (9, 10). Consistent with the well documented anti-apoptotic effect of NF-κB, high levels of NF-κB activity are detectable in various human tumors (11). On the other hand, NF-κB activation results in the promotion of apoptosis, depending on different stimuli and cell types. Huang and Fan (12) reported that the activation of NF-κB contributes to paclitaxel-induced apoptosis in human solid tumor cells. In addition, Bian *et al.* (13) found that NF-κB activation mediates doxorubicin-induced apoptosis in N-type neuroblastoma cells. In both cases, treatment of cells with the cytotoxic agents significantly down-regulated cytoplasmic IκB-α and then promoted the nuclear transloca-

* This work was supported in part by a grant-in-aid for third term comprehensive control research for cancer from the Ministry of Health, Labor and Welfare, by a grant-in-aid for scientific research on priority areas from the Ministry of Education, Culture, Sports, Science and Technology of Japan, and by a grant-in-aid for scientific research from the Japan Society for the Promotion of Science. The costs of publication of this article were defrayed in part by the payment of page charges. This article must therefore be hereby marked "*advertisement*" in accordance with 18 U.S.C. Section 1734 solely to indicate this fact.

[1] To whom correspondence should be addressed: Div. of Biochemistry, Chiba Cancer Center Research Inst., 666-2 Nitona, Chuoh-ku, Chiba 260-8717, Japan. Tel.: 81-43-264-5431; Fax: 81-43-265-4459; E-mail: akiranak@chiba-cc.jp.

[2] The abbreviations used are: IKK, IκB kinase; TNF-α, tumor necrosis factor-α; CDDP, cisplatin; siRNA, small interfering RNA; MEFs, mouse embryonic fibroblasts; MTT, 3-(4,5-dimethylthiazol-2-yl)-2,5-diphenyltetrazolium bromide; RT, reverse transcription; GST, glutathione *S*-transferase; HA, hemagglutinin; PIPES, 1,4-piperazinediethanesulfonic acid; MOPS, 4-morpholinepropanesulfonic acid; CBP, cAMP-responsive element-binding protein-binding protein.

tion of NF-κB; however, the molecular mechanism of the pro-apoptotic effect of NF-κB is still largely unknown.

p73 belongs to a small family of p53-related nuclear transcription factors. In accordance with their structural similarity, p73 functions in a manner analogous to p53 by inducing G_1 cell cycle arrest or apoptosis in certain cancerous cells through transactivating an overlapping set of p53/p73 target genes (reviewed in Ref. 14). Like p53, endogenous p73 becomes stabilized as well as activated in cells exposed to certain genotoxic stimuli, including γ-irradiation and cisplatin (CDDP), and contributes to an apoptotic response to DNA damage (15–17). p73 is expressed as multiple isoforms that differ at their N and C termini, arising from alternative splicing and promoter usage (reviewed in Ref. 14). Among them, an N-terminally truncated form of p73 (ΔNp73) that lacks the transactivation domain of p73 has an oncogenic potential and exhibits dominant-negative behavior toward wild-type p73 as well as p53 (18–20). Of particular note, we (22) and others (21, 23) demonstrated that p73 directly transactivates the expression of its own negative regulator, ΔNp73, suggesting that a negative feedback regulation of p73 by ΔNp73 exists to modulate cell survival and death.

In response to primary antigenic stimulation, NF-κB limits the up-regulation of pro-apoptotic p73 in T cells, resulting in the promotion of T cell survival; however, the precise molecular basis by which NF-κB activation inhibits the expression of p73 remains to be determined (24). It is worth noting that IKK-β, but not IKK-α, activates NF-κB, thereby inhibiting the accumulation of p53 at the protein level in response to the anticancer agent doxorubicin (25). IκB-α might play a role in sequestering p53 in the cytoplasm through the physical interaction with p53, thereby preventing the nuclear translocation of p53 (26). These observations suggest that NF-κB activation might abrogate p53- and/or p73-mediated apoptosis. In marked contrast, Ryan *et al.* (27) reported that NF-κB is required for p53-dependent apoptosis. Additionally, it has been demonstrated that p53 is a direct transcriptional target of NF-κB and that the p53-activating signal is partially blocked by inhibition of NF-κB activation (28–30). In support of this notion, Fujioka *et al.* (31) reported that NF-κB acts as a pro-apoptotic factor by activating the p53 signaling pathway. However, the functional significance of the possible interplay between the NF-κB signaling pathway and p53- and/or p73-mediated apoptosis has not been established.

In addition to the role of the cytoplasmic IKK complex in regulating the signal-dependent induction of NF-κB target genes, Birbach *et al.* (32) found that one of its components (IKK-α) shuttles between the cytoplasm and nucleus of unstimulated cells, suggesting that IKK-α might have a novel nuclear role in controlling cell survival and death. Consistent with this notion, it has been shown that IKK-α accumulates in the cell nucleus in response to cytokine exposure and stimulates the expression of NF-κB-responsive genes through promoter-associated histone H3 phosphorylation (33, 34). In this study, we found that IKK-α accumulates in the cell nucleus during the CDDP-mediated apoptotic process. Moreover, IKK-α increased the stability of p73, but not p53, through direct interaction with p73 and enhanced p73-dependent transcriptional activity as well as pro-apoptotic function. Reduction of endogenous IKK-α by small interfering RNA (siRNA) against IKK-α resulted in the significant attenuation of the CDDP-induced accumulation of p73α. Similar results were also obtained in mouse embryonic fibroblasts (MEFs) derived from IKK-α-deficient mice (IKK-$\alpha^{-/-}$ MEFs). Thus, our findings suggest that IKK-α has a novel nuclear role in regulating DNA damage-induced apoptosis, which is distinct from its cytoplasmic role in activating NF-κB.

EXPERIMENTAL PROCEDURES

Cell Lines and Transfection—African green monkey kidney COS-7 cells and human osteosarcoma U2OS cells were maintained in Dulbecco's modified Eagle's medium, 10% fetal bovine serum, penicillin, and streptomycin (Invitrogen). Human lung carcinoma H1299, human neuroblastoma SK-N-AS, and mouse fibrosarcoma L929 cells were grown in RPMI 1640 medium, 10% fetal bovine serum, penicillin, and streptomycin. COS-7 cells were transfected with FuGENE 6 (Roche Applied Science) in accordance with the manufacturer's specifications. H1299 and U2OS cells were transfected with Lipofectamine (Invitrogen) according to the manufacturer's instructions. pcDNA3 (Invitrogen) was used as a blank plasmid to balance the amount of DNA introduced in transient transfection.

Cell Survival Assay—U2OS cells were seeded at 5×10^3/well in a 96-well tissue culture dish with 100 μl of complete medium and allowed to attach overnight. CDDP was added to the cultures at a final concentration of 20 μM, and cell viability was determined by a modified 3-(4,5-dimethylthiazol-2-yl)-2,5-diphenyltetrazolium bromide (MTT) assay at the indicated time points after the addition of CDDP as described (22).

RNA Extraction and Reverse Transcription (RT)-PCR—Total RNA was prepared from U2OS cells exposed to CDDP (20 μM) using an RNeasy mini kit (Qiagen Inc.) according to the manufacturer's protocol. For the RT-PCR, first-strand cDNA was generated using SuperScript II reverse transcriptase (Invitrogen) and random primers. PCR amplification was performed with r*Taq* DNA polymerase (Takara, Ohtsu, Japan).[3] The expression of glyceraldehyde-3-phosphate dehydrogenase was measured as an internal control.

Plasmids—The protein-coding region of IKK-α was amplified by PCR and inserted between the EcoRI and XhoI sites of pcDNA3-FLAG. The K44A mutation was introduced into wild-type IKK-α using PfuUltra™ high fidelity DNA polymerase (Stratagene) according to the manufacturer's instructions. The nucleotide sequence of the PCR product was determined to verify the presence of the desired mutation and the absence of random mutations.

Immunoblotting, Immunoprecipitation, and Glutathione S-Transferase (GST) Pulldown Assay—For immunoblotting, cell lysates (50 μg of protein) were analyzed using anti-FLAG monoclonal antibody M2 (Sigma); anti-hemagglutinin (HA) monoclonal antibody (12CA5, Roche Applied Biosciences); anti-p73 monoclonal antibody (Ab-4, NeoMarkers, Fremont, CA); anti-p53 monoclonal antibody (DO-1, Oncogene Research Products, Cambridge, MA); anti-Bax monoclonal antibody (6A7, eBioscience, San Diego, CA); anti-IKK-α polyclonal (M-280), anti-IKK-β polyclonal (H-470), anti-IKK-γ

[3] The list of primer sets used is available upon request.

polyclonal (FL-417), anti-p65 polyclonal (C-20), anti-IκB-α polyclonal (C-21), or polyclonal anti-$p21^{WAF1}$ (H-164) antibody (Santa Cruz Biotechnology, Inc., Santa Cruz, CA); or anti-actin polyclonal antibody (20–33, Sigma). After incubation with primary antibodies, membranes were incubated with horseradish peroxidase-conjugated secondary antibodies (Cell Signaling Technology, Beverly, MA), and immunoreactive proteins were finally visualized by the ECL system (Amersham Biosciences AB, Uppsala, Sweden). For immunoprecipitation, cell lysates were precleared with 30 μl of protein G-Sepharose suspension (Amersham Biosciences AB) and then incubated with anti-HA polyclonal antibody (Medical and Biological Laboratories, Nagoya, Japan) or anti-FLAG monoclonal antibody for 2 h at 4 °C. Immunoblotting was performed with anti-FLAG or anti-p73 monoclonal antibody as described above. For GST pulldown assay, [^{35}S]methionine-labeled FLAG-IKK-α was generated in the coupled transcription/translation system (Promega, Madison, WI) and mixed with GST or GST-p73 fusion proteins coupled to glutathione-Sepharose (Amersham Biosciences AB) for 2 h at 4 °C. ^{35}S-Labeled bound proteins were analyzed by 10% SDS-PAGE and visualized by autoradiography.

Subcellular Fractionation and Immunofluorescence Analysis—To prepare nuclear and cytoplasmic extracts, cells were lysed in 10 mM Tris-HCl (pH 7.5), 1 mM EDTA, 0.5% Nonidet P-40, 1 mM phenylmethylsulfonyl fluoride, and a protease inhibitor mixture (Sigma) and centrifuged at 5000 rpm for 10 min to collect soluble fractions, which are referred to as cytosolic extracts. Insoluble materials were washed with the lysis buffer and further dissolved in SDS sample buffer to collect the nuclear extracts. The nuclear and cytoplasmic fractions were subjected to immunoblot analysis using anti-lamin B monoclonal antibody (Ab-1; Oncogene Research Products) or anti-α-tubulin monoclonal antibody (DM1A, Cell Signaling Technology). For indirect immunofluorescence, U2OS cells were grown on coverslips and transfected with the indicated expression plasmids. Forty-eight hours after transfection, cells were fixed in 100% methanol for 20 min at −20 °C, blocked in 3% bovine serum albumin, stained with the corresponding antibodies, and examined with a laser scanning confocal microscope (Olympus, Tokyo, Japan). Nuclear matrix fractionation was performed as described previously (35, 36). In brief, cells were washed with ice-cold phosphate-buffered saline and lysed in 10 mM PIPES (pH 6.8), 100 mM NaCl, 300 mM sucrose, 3 mM $MgCl_2$, 1 mM EGTA, 1 mM dithiothreitol, and 0.5% Triton X-100 containing a protease inhibitor mixture, and insoluble materials were separated from soluble proteins (fraction I) by centrifugation. The pellet fraction was treated with DNase I (at a final concentration of 1 mg/ml) for 15 min at 37 °C, and then ammonium sulfate was added to the reaction mixture (at a final concentration of 0.25 M). The pellet fraction was separated from the supernatant (fraction II) by centrifugation and further extracted with 2 M NaCl (fraction III). The remaining pellet was solubilized in 8 M urea, 0.1 M NaH_2PO_4, and 10 mM Tris-HCl (pH 8.0) to give fraction IV.

Protein Stability and Ubiquitination Assays—COS-7 cells were transfected with HA-p73α with or without IKK-α. Cells were harvested at different time points after pretreatment with cycloheximide (100 μg/ml), and cell lysates were processed for immunoblot analysis with anti-p73 or anti-actin antibody. Densitometry was used to quantify the amounts of HA-p73α that normalized to actin. Ubiquitination assay was performed as described previously (37). COS-7 cells were cotransfected with HA-p73α and His-tagged ubiquitin with or without IKK-α. Forty hours after transfection, cells were exposed to the proteasomal inhibitor MG132 (20 μM) for 6 h. Cells were resuspended in 6 M guanidine HCl, 0.1 M Na_2HPO_4/NaH_2PO_4 (pH 8.0), and 10 mM imidazole, and ubiquitinated materials were recovered by nickel-nitrilotriacetic acid-agarose beads (Qiagen Inc.) and analyzed by immunoblotting with anti-HA antibody.

Luciferase Reporter and Apoptosis Assays—p53-deficient H1299 cells on 12-well plates were cotransfected with a p53/p73-responsive element-driven luciferase reporter, an internal control vector for *Renilla* luciferase, and a combination of the indicated expression vectors. Both firefly and *Renilla* luciferase activities were assayed with the Dual-Luciferase reporter assay system (Promega). The firefly luminescence signal was normalized based on the *Renilla* luminescence signal. For apoptosis assay, H1299 cells on 6-well plates were cotransfected with β-galactosidase (50 ng) and HA-p73α (50 ng) with or without increasing amounts of IKK-α or IKK-β (100, 200, and 400 ng). Forty-eight hours after transfection, cells were stained with a 0.4% solution of trypan blue for 10 min at room temperature. Thereafter, cells were fixed in phosphate-buffered saline containing 2.5% glutaraldehyde, 1 mM $MgCl_2$, and 2 mM EGTA for 10 min and then stained with Red-Gal for 2 h as described (11). Red-Gal was used as a marker to visualize the transfected cells and to assess the apoptotic frequency among the transfectants. Apoptotic cells were scored by rounding up of cells with dark pink-purple coloration due to double staining with Red-Gal and trypan blue.

In Vitro Kinase Assay—GST or GST-p73 deletion mutants were incubated with the active form of IKK-α (Upstate Biotechnology, Lake Placid, NY) in a solution containing 40 mM MOPS-NaOH (pH 7.0), 1 mM EDTA, 25 mM sodium acetate, and 0.25 mM ATP in the presence of [γ-^{32}P]ATP at 30 °C for 10 min. After incubation, the reaction mixtures were separated by SDS-PAGE. The gel was then dried and subjected to autoradiography.

RNA Interference—To knock down endogenous IKK-α, the expression plasmid for siRNA directed against human IKK-α (GeneSuppressor, Imgenex Corp., San Diego, CA) was introduced into U2OS cells using Lipofectamine following the manufacturer's instructions. Forty-eight hours after transfection, whole cell lysates were prepared and analyzed for the expression levels of IKK-α by immunoblotting.

Chromatin Immunoprecipitation Assays—Chromatin immunoprecipitation assays were performed following a protocol provided by Upstate Biotechnology (Lake Placid, NY). In brief, cells were cross-linked with 1% formaldehyde in medium for 10 min at 37 °C. Chromatin solutions were prepared and immunoprecipitated with anti-HA antibody. DNAs of the immunoprecipitates and control input DNAs were purified using a QIAquick PCR purification kit (Qiagen Inc.) and then analyzed by regular PCR using human *Bax* promoter-specific

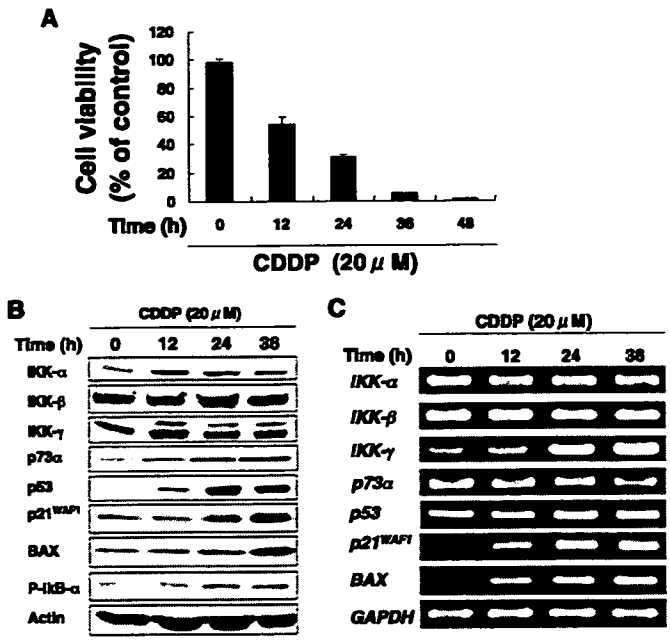

FIGURE 1. **Induction of IKK-α in response to CDDP.** *A*, effect of CDDP on osteosarcoma-derived U2OS cell survival. At the indicated time points after treatment with CDDP (at a final concentration of 20 μM), cell viability was determined by MTT assays. *B*, immunoblot analysis. At the indicated time periods after treatment with CDDP, whole cell lysates were prepared and subjected to immunoblotting with the indicated antibodies. For p73α, whole cell lysates were subjected to immunoprecipitation with anti-p73 antibody, followed by immunoblotting with anti-p73 antibody. Actin expression served as a control for equal loading of proteins in each lane. *C*, RT-PCR analysis. Total RNA was extracted from U2OS cells at the indicated times after CDDP treatment and used for RT-PCR with the indicated primers. Glyceraldehyde-3-phosphate dehydrogenase (*GAPDH*) was used as a control.

primers. The primer sequences used were 5′-AGGCTGAGACG-GGGTTATCT-3′ and 5′-AAAGCTCAGAGGCCCAAAAT-3′.

RESULTS

Induction of IKK-α during CDDP-mediated Apoptosis in U2OS Cells—To define the potential function(s) of IKKs in DNA damage-induced signaling, we first examined their expression levels in human osteosarcoma-derived U2OS cells exposed to the DNA-damaging chemotherapeutic drug CDDP. Under our experimental conditions, U2OS cells underwent apoptosis in a time-dependent manner as examined by cell survival assays (Fig. 1*A*). Similar results were also obtained by fluorescence-activated cell sorter analysis (data not shown). Immunoblot analysis demonstrated that p53 and its homolog p73α, which are major mediators in the DNA damage response (reviewed in Refs. 14 and 38), were significantly induced at protein levels in response to CDDP (Fig. 1*B*), whereas the expression of *p53* and *p73α* mRNAs remained unchanged (Fig. 1*C*). Their accumulation was associated with several of their downstream effectors, including $p21^{WAF1}$ and Bax. Notably, CDDP treatment led to a remarkable accumulation of IKK-α, and its induction was observed between 12 and 36 h after exposure to CDDP (Fig. 1*B*). Twelve hours after treatment with CDDP, the amount of IKK-γ (NEMO) was transiently increased at the protein level. By contrast, the amount of IKK-β was not significantly altered upon CDDP treatment.

RT-PCR analysis revealed that the expression levels of *IKK-α* and *IKK-β* mRNAs remained unchanged regardless of CDDP treatment, whereas a marked increase in the expression level of *IKK-γ* mRNA was detected in a time-dependent manner in response to CDDP (Fig. 1*C*). Intriguingly, immunoblot analysis also demonstrated that CDDP treatment caused a significant increase in the phosphorylated form of IκB-α, which is a well characterized substrate for the IKK complex (reviewed in Ref. 3). Taken together, these results suggest that DNA damage-induced accumulation of both p53 and p73α is associated with the up-regulation of IKK-α and IKK-γ and that a functional interaction might exist between them in DNA damage-mediated apoptotic pathways.

Nuclear Accumulation of IKK-α in Response to CDDP—It was shown recently that IKK-α shuttles between the nucleus and cytoplasm in a CRM1-dependent fashion (32). Nuclear IKK-α has the ability to transactivate NF-κB-responsive genes that control survival pathways after cytokine exposure (33, 34). In addition, Verma *et al.* (39) found that, like IKK-α, IKK-γ is present in both the nucleus and cytoplasm. These observations prompted us to examine whether the subcellular localization of endogenous IKKs can change in response to CDDP. For this purpose, nuclear and cytoplasmic extracts were prepared from U2OS cells exposed to CDDP or left untreated and then subjected to immunoblotting with the indicated antibodies. In agreement with previous results (33), IKK-α was localized in both the nucleus and cytoplasm, whereas IKK-β was expressed almost exclusively in the cytoplasm (Fig. 2*A*). The amounts of cytoplasmic IKK-α, IKK-β, and IKK-γ remained unchanged regardless of the treatment with CDDP. Of note, CDDP treatment led to a remarkable accumulation of IKK-α in the cell nucleus in a time-dependent manner, whereas IKK-β accumulated in the cell nucleus to a lesser degree. The temporal patterns of CDDP-mediated accumulation of nuclear IKK-α correlated with those of p73α. On the other hand, the transient nuclear accumulation of IKK-γ was detected 12 h after exposure to CDDP. Compared with the levels of nuclear IKK-α accumulated in response to CDDP, the amount of nuclear IKK-γ was small. Consistent with the enhanced phosphorylation of IκB-α in response to CDDP, cytoplasmic IκB-α was decreased in a time-dependent manner. However, CDDP treatment had little or no effect on the nuclear accumulation of the NF-κB p65 subunit (RelA), indicating that nuclear translocation of p65 might be inhibited in the presence of CDDP. Considering that, among IKKs, CDDP treatment promoted a significant nuclear accumulation of IKK-α, it is likely that IKK-α might have a certain nuclear function during CDDP-mediated apoptosis.

To investigate whether exogenously expressed IKK-α can reflect the behavior of endogenous IKK-α, we examined the intracellular distribution of exogenous IKK-α by immunoblotting and immunofluorescence staining. Nuclear and cytoplasmic fractions were prepared from U2OS cells transfected with the expression plasmid for FLAG-IKK-α or HA-p73α and subjected to immunoblotting with anti-FLAG or anti-p73α antibody, respectively. As shown in Fig. 2*B*, HA-p73α was localized exclusively in the cell nucleus, whereas FLAG-IKK-α was present in both the nucleus and cytoplasm. Surprisingly, immunofluorescence staining with anti-FLAG and anti-lamin B antibodies clearly showed that exogenous IKK-α was localized in